tallographic characterization of a purified HEV-$VLP_{ORF3/ORF2}$ capsid composed of a fusion protein obtained by inserting a fragment of ORF3 (residues 70–123) at the N-terminus of the ORF2 peptide including residues 112–608.

2. Experimental procedures and results

2.1. Expression and purification of recombinant HEV-VLPs

Recombinant HEV-$VLP_{ORF3/ORF2}$ was produced using a similar approach to those described previously (Li *et al.*, 1997; Xing *et al.*, 1999) except that an ORF3/ORF2 fusion protein containing a fragment of the ORF3 protein (residues 70–123) attached without an intervening sequence to the N-terminus of a truncated ORF2 protein (residues 112–608) was used in the construct for expression. The transfer vector was co-transfected with insect Sf9 cells (Riken Cell Bank, Tsukuba, Japan) to produce the recombinant baculovirus. The recombinant baculovirus obtained was plaque-purified three times. For large-scale expression, an insect-cell line from *Trichoplusia ni*, BTL-Tn 5B1-4 (Tn5; Invitrogen, San Diego, California, USA), was used and was infected with recombinant baculovirus at a multiplicity of infection of 10. The cells were incubated in EX-CELL-405 medium (JRH Biosciences, Lenexa, Kansas, USA) for 7 d at 300 K. The VLPs were harvested from the supernatant. The recombinant baculovirus and cell debris were removed by centrifugation at 10 000*g* for 90 min at 277 K. The VLPs in the supernatant were then spun down at 100 000*g* for 2 h at 277 K. The resulting VLP pellets were then resuspended in EX-CELL-405 medium and further purified in a CsCl equilibrium density gradient. On inspection by negative-staining EM, the morphology of $VLP_{ORF3/ORF2}$ appeared to be similar to that of VLP_{ORF2}, except for an extra density within the particles.

Prior to crystallization or cryo-electron microscopy (EM) experiments, the purified VLPs were pelleted through a 5%(*w*/*v*) sucrose cushion in 50 m*M* potassium–MES buffer pH 6.2 at 110 000*g* in a Beckman SW 55-Ti rotor at 277 K for 1 h. The pellet was resuspended in 50 m*M* potassium–MES buffer pH 6.2 and maintained at 277 K for 10 min. The concentration of recombinant HEV-VLP was adjusted to 10 mg ml^{-1} according to the standard concentration curve determined from the light absorbance at 260 and 280 nm. The quality of the purified particles was routinely verified by EM using 2%(*w*/*v*) uranyl acetate negative-stain contrast (Agar Scientific Ltd, Stansted, England) and SDS–PAGE performed on 8–25% acrylamide gels under denaturing conditions (Gong *et al.*, 1990; Cheng *et al.*, 1992).

2.2. Cryo-EM and three-dimensional reconstruction of purified $VLP_{ORF3/ORF2}$

Cryo-EM sample preparation followed previously established procedures (Xing *et al.*, 1999). Briefly, a 3.5 µl drop of $VLP_{ORF3/ORF2}$ suspension was applied onto a glow-discharged 'holey' carbon-coated grid, blotted with filter paper and vitrified by rapidly plunging the grids into liquid ethane cooled by liquid nitrogen. The grids, with the frozen $VLP_{ORF3/ORF2}$ physically fixed to fill in the holes of the carbon film after rapid freezing, were transferred to an FEI CM-120 microscope using a Gatan 626DH cryoholder and all subsequent steps were carried out with the sample maintained at 95 K. The electron microscope was operated at 120 kV and low-dose (<7 e^{-} $Å^{-2}$) images were recorded on Kodak SO163 films at a magnification of 45 000×. Selected micrographs with a defocus level of 1000 nm were digitized using a Zeiss microdensitometer (*Z*/*I* imaging) at a step size of 14 µm, which corresponds to 3.1 Å per pixel at the level of the specimen. The first zero of the contrast transfer function was at a spatial frequency of ~0.056 $Å^{-1}$. Isolated VLP images were extracted from the digitized micrographs, normalized and combined into one single image-stacked file for subsequent processing. Determination of the structure was carried out using a model-based polar Fourier transform (PFT) method (Cheng *et al.*, 1994; Baker & Cheng, 1996). As the PFT algorithm requires a three-dimensional model to start with, a cryo-EM density map of VLP_{ORF2} was used as an initial model (Xing *et al.*, 1999). The model was low-pass filtered to 40 Å resolution in order to reduce the influence of noise bias included in image processing. The starting model was back-projected at 1° angular increments to create an image database that covered all possible views of the model at the orientations within one half of the icosahedral asymmetric unit. Individual unique views of model projections in the database were interpolated onto a polar grid to form a polar projection (PRJ) image and the PRJ image was then Fourier transformed to produce a PFT image; these PRJ and PFT images were stored in two separate files for use as references for alignment with individual images of PFTs and PRJs from the selected VLP projections (Cheng *et al.*, 1994; Baker & Cheng, 1996). In addition, the alignment was performed with enhanced accuracy by initially including a band-pass filter (spatial frequency between 1/90 $Å^{-1}$ and 1/30 $Å^{-1}$) of the PFT images to optimize the search for origins and orientations. A list of origins and orientations corresponding to each particle was obtained and a noise-filtered three-dimensional reconstruction was computed using the Fourier–Bessel algorithm implemented with a cylinder expansion method and imposed 522 symmetry (Crowther, 1971; Cheng *et al.*, 1992; Fuller *et al.*, 1996). The presence of the threefold symmetry in the three-dimensional model validated the accuracy of the reconstruction. The search model was subsequently updated with the newly computed three-dimensional density map of $VLP_{ORF3/ORF2}$ through individual cycles of refinement to make the orientations and origins of the image data to be included in the averaging of the subsequent density maps more accurate. The cryo-EM structural density of $VLP_{ORF3/ORF2}$ for use in initial phasing of the X-ray diffraction data was achieved by the progressive addition of data at higher spatial frequency. The iterations were continued by re-projecting the model at a finer angular increment (0.5°) and by progressively extending the low-pass filter from 30 to 20 Å. The cycles of refinement stopped when no major improvement was observed in the three-dimensional reconstruction. Fourier shell correlations of the reconstruction yielded an estimated resolution of 24 Å for recombinant HEV-$VLP_{ORF3/ORF2}$ based on Fourier averaging of 134 VLP images (Fig. 1). $VLP_{ORF3/ORF2}$ has a diameter of ~270 Å and the capsid shell was composed of 30 dimer-like protrusions arranged in a $T = 1$ icosahedral surface lattice. Analysis of the density-distribution map revealed $VLP_{ORF3/ORF2}$ to consist of 60 subunits of the fusion protein. The VLP structure demonstrated two distinct domains, namely the shell domain, which forms a continuous layer of viral capsid, and the protrusion domain, which forms protruding spikes (Cheng *et al.*, 1992, 1995). The cryo-EM density map of $VLP_{ORF3/ORF2}$ was subsequently used for initial phasing of the data collected by X-ray diffraction.

2.3. Crystallization strategy and data collection

The initial crystallization trials were performed by the hanging-drop method (McPherson, 2004*a*,*b*) with a commercially available kit, Crystal Screen Lite, from Hampton Research (Laguna Niguel, California, USA) at 293 K. The crystallization drops contained 2 µl $VLP_{ORF3/ORF2}$ solution at various concentrations mixed with 2 µl screening solution and were set up for vapor diffusion against 1 ml screening solution in 24-well plates (Falcon). Crystals were obtained using two different conditions: (i) 4%(*w*/*v*) polyethylene glycol (PEG) 4000 in 100 m*M* sodium acetate pH 4.6 and (ii) 4%(*w*/*v*) PEG

8000 in 100 m*M* Tris–HCl pH 8.5. In condition (i) a number of small crystals appeared within a few minutes, while in condition (ii) the crystals appeared after one week. To further assess the integrity of the VLPs packed in the crystals, we selected crystals from both the pH 4.6 and pH 8.5 conditions, dissolved them in the respective reservoir solution and performed negative-staining EM with 2%(*w*/*v*) uranyl acetate (Gong *et al.*, 1990). The VLPs had remained intact within the crystals in both conditions (Fig. 2). The quality of these crystals was assessed using an in-house X-ray generator. The crystals obtained at pH 4.6 diffracted to a lower resolution (40 Å) compared with those obtained at pH 8.5 (20 Å). Based on this result, the crystallization conditions were further optimized by changing the PEG 8000 and VLP concentrations. Good-quality crystals were obtained with 3.5%(*w*/*v*) PEG 8000 in 100 m*M* Tris–HCl pH 8.5; these crystals were rod-shaped and reached a maximum length of 1 mm after 14 d (Fig. 3).

The HEV-VLP$_{ORF3/ORF2}$ crystals were immersed for 2 min in reservoir solution containing 20, 30 or 40%(*v*/*v*) ethylene glycol as a cryoprotectant. A single crystal was picked up with a cryoloop and directly flash-frozen in liquid nitrogen. The HEV-VLP$_{ORF3/ORF2}$ crystals were found to be very fragile and cracked in most cases. Therefore, the VLPs were subsequently crystallized under the same conditions with the addition of 20–40%(*v*/*v*) ethylene glycol to the reservoir. The crystals obtained had a similar appearance to those obtained without the addition of ethylene glycol. One of the resulting crystals was successfully frozen and diffracted X-rays to beyond 7.8 Å resolution at 100 K on a DIP6040 imaging-plate/CCD hybrid detector (MacScience, Bruker-AXS) with a crystal-to-detector distance of 700 mm, an oscillation angle of 1.0° and an exposure time of 10 s using synchrotron radiation at SPring-8 (Hyogo, Japan) beamline BL44XU (Fig. 4). As the crystal decayed during data collection, the data set was only processed to 8.3 Å resolution. The diffraction images were indexed, reduced, scaled and merged using the *HKL-2000* package (Otwinowski & Minor, 1997). The intensities were converted into the structure-factor amplitudes using *TRUNCATE* from the *CCP*4 package (Collaborative Computational Project, Number 4, 1994). The space group was determined to be $P2_12_12_1$ by scaling in the resolution range 70–8.3 Å assuming Laue group 222 (R_{merge} = 13.6% from *SCALEPACK*) and was assigned on the basis of systematic absences of odd reflections along the *h*00, 0*k*0 and 00*l* axes. The unit-cell parameters were a = 337, b = 343, c = 346 Å, $\alpha = \beta = \gamma = 90°$. The statistics of data collection are summarized in Table 1. The value of $I/\sigma(I)$ was found to be 8.3 and 2.2 for the resolution ranges 70–8.3 and 8.6–8.3 Å, respectively. The R_{merge} for the outermost resolution shell was slightly worse than for most low-symmetry protein structure determinations. In this case of viral crystallography, the additional noncrystallographic averaging (60-fold) and the solvent flattening provided the phasing power required to successfully employ the diffraction data to 8.3 Å resolution. While four particles were found in one unit cell (with a molecular weight of 3.2 × 10^6 Da), there is only one complete VLP per

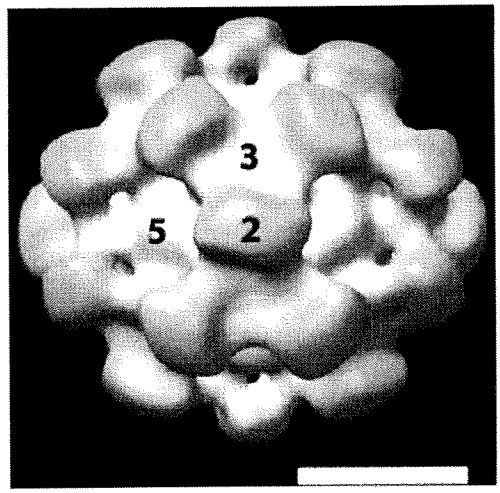

Figure 1
Three-dimensional structure of recombinant HEV-VLP$_{ORF3/ORF2}$ at a resolution of 24 Å determined by cryo-EM and image reconstruction. An isosurface representation of the outer surface of recombinant HEV-VLP$_{ORF3/ORF2}$ is shown viewed along the icosahedral twofold axis. The surface density was contoured at a level corresponding to 100% mass of the expected particle volume. The particle is color-coded to differentiate two distinct domains: the shell domain (white) and the protrusion domain (yellow). The surface capsid conforms to T = 1 icosahedral symmetry in which the 60 subunits are arranged into 30 protruding spikes with the homodimers as the basic building blocks at each icosahedral twofold axis. The scale bar represents 100 Å.

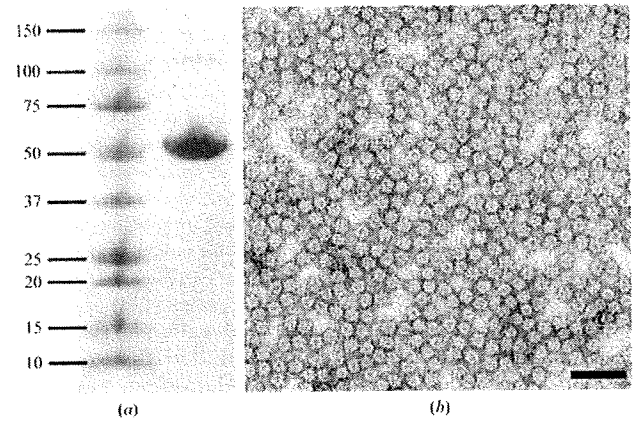

Figure 2
Purity and integrity of recombinant HEV-VLP$_{ORF3/ORF2}$ crystals grown in 4%(*w*/*v*) PEG 8000, 100 m*M* Tris–HCl pH 8.5 analyzed by SDS–PAGE (*a*) and negative-stained electron microscopy (*b*). In (*a*), the left lane contains molecular-weight markers (kDa) and the right lane contains the protein band of recombinant HEV-VLP from a dissolved crystal. In (*b*), a recombinant HEV-VLP$_{ORF3/ORF2}$ crystal was crushed with a nylon loop and stained with 2% uranyl acetate; the VLPs remained with intact capsid morphology after dissolving from the crystal. The bar represents 1000 Å.

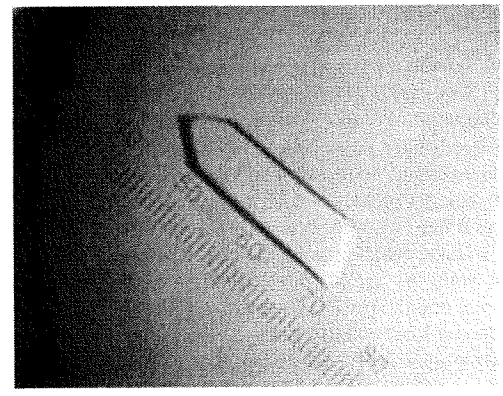

Figure 3
Recombinant HEV-VLP$_{ORF3/ORF2}$ crystal. The crystal was grown in Tris–HCl pH 8.5 buffer, 3.5%(*w*/*v*) PEG 8000 with the addition of 30% ethylene glycol as a cryoprotectant. In the scale, 28 intervals represent 0.1 mm.

asymmetric unit, resulting in 60-fold noncrystallographic symmetry redundancy. The calculated Matthews coefficient V_M is 3.1 Å^3 Da^{-1} (Matthews, 1968).

2.4. Phase determination

A self-rotation function was computed using the program *POLARRFN* from the *CCP*4 package in order to determine the orientation of the icosahedral noncrystallographic symmetry elements. By using reflections in the resolution range 15–10 Å, a fast rotation function was calculated with an integration radius of 130 Å and a B factor of −70 Å^2. The section corresponding to the fivefold axis is depicted in Fig. 5(*a*). The fivefold rotation function was consistent with the presence of four particles per unit cell. Six peaks were clearly identified corresponding to one of the four particles in the unit cell. While additional peaks were observed corresponding to the symmetry-related particles, some unexpected peaks might arise from the 72° rotational relationship between the icosahedral particles, as they were reproduced from the calculated data using a cryo-EM map. Subsequently, the molecular-replacement method starting from a cryo-EM density map (Fig. 1) was used to phase the reflections. The original cryo-EM map was rotated to superimpose the icosahedral symmetry axes of the cryo-EM density onto the VLP orientation determined by the rotation function using the matrix

$$\begin{pmatrix} 0.901271 & -0.269099 & -0.339552 \\ 0.311789 & 0.947022 & 0.077054 \\ 0.300829 & -0.175315 & 0.937426 \end{pmatrix}.$$

Packing considerations suggested that the particle is situated close to the positions in space group $P2_12_12_1$ with $x = 0$, $y = 0$, $z = 0$ or $x = 0.25$,

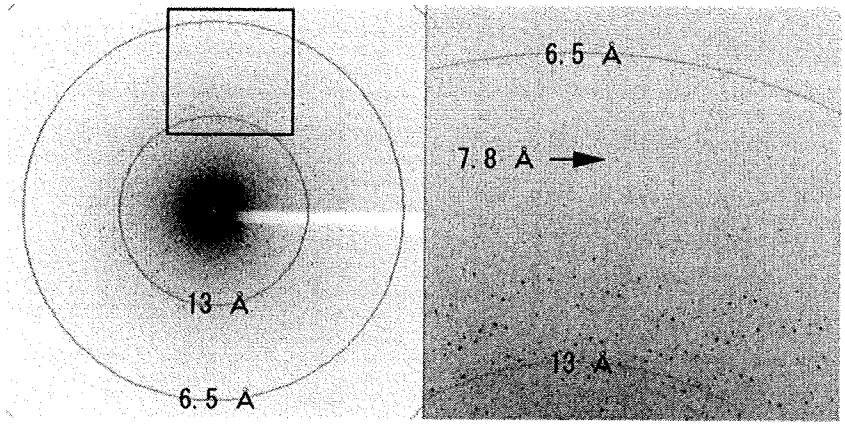

(*a*) (*b*)

Figure 4
A diffraction pattern recorded from a recombinant HEV-VLP$_{ORF3/ORF2}$ crystal. (*a*) A typical 1.0° oscillation photograph exposed for 10 s. The concentric circles indicate the 13.0 and 6.5 Å resolution shells. (*b*) An enlarged image shows a diffraction spot observed at 7.8 Å (indicated by an arrow).

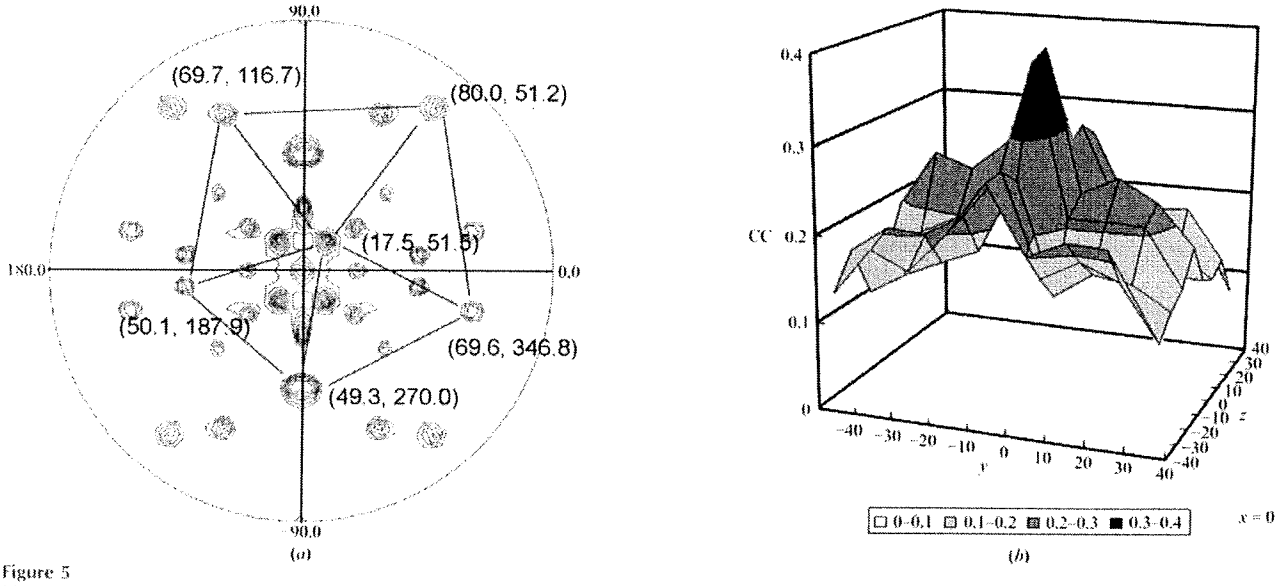

(*a*) (*b*)

Figure 5
Phasing X-ray data with a cryo-EM density map. (*a*) Fivefold self-rotation function peaks calculated in *POLARRFN* with data in the resolution range 15–10 Å and a radius of integration of 130 Å. The positions (φ, ψ) corresponding to one of the four particles in the unit cell are indicated. (*b*) Translational correlation coefficient search for the origin of recombinant HEV-VLP$_{ORF3/ORF2}$. The data used in the calculations were in the resolution range 70–30 Å (only the result at $x = 0$ is shown). The search grid started at the coarse interval of 10 Å and was refined at a finer interval of 2 Å. The maximum correlation coefficient was observed at the point (−2, 0, −6 Å).

Table 1
Crystal information and data-processing statistics.

Values in parentheses are for the outermost shell.

Space group	$P2_12_12_1$
Unit-cell parameters (Å, °)	$a = 337$, $b = 343$, $c = 346$, $\alpha = \beta = \gamma = 90$
Resolution range (Å)	70.00–8.30 (8.60–8.30)
Wavelength (Å)	0.9
Total No. of crystals	1
Total No. of reflections	101760
Unique reflections	33414 (3347)
Completeness (%)	87.6 (89.4)
Multiplicity	3.0 (3.0)
$I/\sigma(I)$	8.3 (2.2)
R_{merge}†	0.136 (0.500)

† $R_{merge} = \sum_{hkl}\sum_i |I_i(hkl) - \langle I(hkl)\rangle| / \sum_{hkl}\sum_i I_i(hkl)$, where $I_i(hkl)$ is the intensity of an individual measurement of the reflection hkl and $\langle I(hkl)\rangle$ is the mean intensity for all measurements including symmetry equivalents.

$y = 0.25$, $z = 0.25$. The correlation coefficient was computed between the structure factors observed from the amplitudes of the X-ray diffraction data (F_o) and the amplitudes of the calculated structure factor (F_c) derived from Fourier transformation of the cryo-EM model properly rotated and positioned in the crystal unit cell around these two positions using the programs *MAVE* from the *RAVE* package of the Uppsala Software Factory (Kleywegt *et al.*, 2001) and *SFALL* and *RSTATS* from the *CCP*4 package. The translation search was initially carried out with a coarse interval of 10 Å steps using data in the resolution range 70–30 Å. After searching with a finer interval of 2 Å, a maximum correlation coefficient value of 0.41 was reached at the origin (−2, 0, −6 Å) (Fig. 5*b*). Phase refinement and extension were carried out in the resolution range 30–8.3 Å using real-space averaging and solvent flattening with the *RAVE* and *CCP*4 packages as performed in our previous work (Nakagawa *et al.*, 2003). The final correlation coefficient and R factor between the F_os and the F_cs obtained from inversion of the averaged and solvent-flattened map at 8.3 Å resolution were 0.92 and 0.21, respectively.

3. Conclusion

We report here the detailed conditions for the crystallization of recombinant HEV-VLP$_{ORF3/ORF2}$ and the implementation of a 24 Å cryo-EM density map in the initial phasing of the X-ray diffraction data. The diffraction data presented carry sufficient information for determining the density map of a 270 Å diameter VLP$_{ORF3/ORF2}$ to a resolution of 8.3 Å. The availability of data with improved resolution provides the structural information needed for the better understanding of virus-particle assembly and will be very valuable for HEV vaccine design.

We thank Drs Andy Fisher and Lena Hammar for their critical editing of the manuscript. This project was supported by grants from Cancer Research Center, Swedish Research Council and EC/FP6 Levmac (RHC). C-YW, NM and LX were supported by grants from Cancer Research, STINT Foundation and Discovery Programs, respectively. Part of the data-analysis scheme developed in this study was supported by the National Institutes of Health through the NIH Roadmap for Medical Research (PN2EY018230). C-YW and NM were initially supported as exchange students by the NYMU International Competitiveness Grant and a Grant-in-Aid for 21st Century Centers of Excellence Program, respectively. This article is part of the requirement for the PhD degree fulfilment of C-YW and TY.

References

Baker, T. S. & Cheng, R. H. (1996). *J. Struct. Biol.* **116**, 120–130.
Cheng, R. H., Kuhn, R. J., Olson, N. H., Rossmann, M. G., Choi, H. K., Smith, T. J. & Baker, T. S. (1995). *Cell*, **80**, 621–630.
Cheng, R. H., Olson, N. H. & Baker, T. S. (1992). *Virology*, **186**, 655–668.
Cheng, R. H., Reddy, V. S., Olson, N. H., Fisher, A. J., Baker, T. S. & Johnson, J. E. (1994). *Structure*, **2**, 271–282.
Collaborative Computational Project, Number 4 (1994). *Acta Cryst.* D**50**, 760–763.
Crowther, R. A. (1971). *Philos. Trans. R. Soc. Lond. B Biol. Sci.* **261**, 221–230.
Fuller, S. D., Butcher, S. J., Cheng, R. H. & Baker, T. S. (1996). *J. Struct. Biol.* **116**, 48–55.
Gong, Z. X., Wu, H., Cheng, R. H., Hull, R. & Rossmann, M. G. (1990). *Virology*, **179**, 941–945.
Kleywegt, G. J., Zou, J.-Y., Kjeldgaard, M. & Jones, T. A. (2001). *International Tables for Crystallography*, Vol. *F*, edited by E. Arnold & M. G. Rossmann, pp. 354–355. Dordrecht: Kluwer Academic Publishers.
Li, T. C., Suzaki, Y., Ami, Y., Dhole, T. N., Miyamura, T. & Takeda, N. (2004). *Vaccine*, **22**, 370–377.
Li, T. C., Takeda, N., Miyamura, T., Matsuura, Y., Wang, J. C., Engvall, H., Hammar, L., Xing, L. & Cheng, R. H. (2005). *J. Virol.* **79**, 12999–13006.
Li, T. C., Yamakawa, Y., Suzuki, K., Tatsumi, M., Razak, M. A., Uchida, T., Takeda, N. & Miyamura, T. (1997). *J. Virol.* **71**, 7207–7213.
McPherson, A. (2004*a*). *J. Struct. Funct. Genomics*, **5**, 3–12.
McPherson, A. (2004*b*). *Methods*, **34**, 254–265.
Maloney, B. J., Takeda, N., Suzaki, Y., Ami, Y., Li, T. C., Miyamura, T., Arntzen, C. J. & Mason, H. S. (2005). *Vaccine*, **23**, 1870–1874.
Matthews, B. W. (1968). *J. Mol. Biol.* **33**, 491–497.
Meng, J., Dai, X., Chang, J. C., Lopareva, E., Pillot, J., Fields, H. A. & Khudyakov, Y. E. (2001). *Virology*, **288**, 203–211.
Nakagawa, A., Miyazaki, N., Taka, J., Naitow, H., Ogawa, A., Fujimoto, Z., Mizuno, H., Higashi, T., Watanabe, Y., Omura, T., Cheng, R. H. & Tsukihara, T. (2003). *Structure*, **11**, 1227–1238.
Otwinowski, Z. & Minor, W. (1997). *Methods Enzymol.* **276**, 307–326.
Panda, S. K., Thakral, D. & Rehman, S. (2007). *Rev. Med. Virol.* **17**, 151–180.
Purcell, R. H. & Emerson, S. U. (2008). *J. Hepatol.* **48**, 494–503.
Schofield, D. J., Glamann, J., Emerson, S. U. & Purcell, R. H. (2000). *J. Virol.* **74**, 5548–5555.
Shrestha, M. P. *et al.* (2007). *N. Engl. J. Med.* **356**, 895–903.
Xing, L., Kato, K., Li, T., Takeda, N., Miyamura, T., Hammar, L. & Cheng, R. H. (1999). *Virology*, **265**, 35–45.

J Gastroenterol 2007; 42:411–423
DOI 10.1007/s00535-007-2030-3

Journal of Gastroenterology

Review

Molecular biology of hepatitis C virus

TETSURO SUZUKI, HIDEKI AIZAKI, KYOKO MURAKAMI, IKUO SHOJI, and TAKAJI WAKITA

Department of Virology II, National Institute of Infectious Diseases, 1-23-1 Toyama, Shinjuku-ku, Tokyo 162-8640, Japan

Infection with hepatitis C virus (HCV), which is distributed worldwide, often becomes persistent, causing chronic hepatitis, cirrhosis, and hepatocellular carcinoma. For many years, the characterization of the HCV genome and its products has been done by heterologous expression systems because of the lack of a productive cell culture system. The development of the HCV replicon system is a highlight of HCV research and has allowed examination of the viral RNA replication in cell culture. Recently, a robust system for production of recombinant infectious HCV has been established, and classical virological techniques are now able to be applied to HCV. This development of reverse genetics-based experimental tools in HCV research can bring a greater understanding of the viral life cycle and pathogenesis of HCV-induced diseases. This review summarizes the current knowledge of cell culture systems for HCV research and recent advances in the investigation of the molecular virology of HCV.

Key words: hepatitis C virus, translation, polyprotein processing, RNA replication, viral assembly, ubiquitin

Introduction

Hepatitis C virus (HCV), discovered in 1989, is a major etiologic agent of posttransfusion- and sporadic non-A, non-B hepatitis[1] and at present infects approximately 200 million people worldwide.[2,3] Persistent infection with HCV is associated with the development of chronic hepatitis, hepatic steatosis, cirrhosis, and hepatocellular carcinoma.[3,4–8] HCV is a small, enveloped RNA virus that belongs to the *Hepacivirus* genus of the *Flaviviridae* family.[9,10] Its genome consists of a single-strand of positive-sense RNA of approximately 9.6 kb, which contains an open reading frame (ORF) coding for a polyprotein precursor of approximately 3000 residues.[11] The precursor is cleaved into at least ten different proteins: the structural proteins core, E1, E2, and p7, and the nonstructural proteins NS2, NS3, NS4A, NS4B, NS5A, and NS5B (Fig. 1).

To date, six major genotypes of HCV have been identified that differ by 31%–34% in their nucleotide sequence and by about 30% in their amino acid sequence. It has been shown that HCV, like many other RNA viruses, circulates in infected individuals as a population of diverse but closely related variants referred to as quasispecies.[12] This quasispecies model of mixed virus populations may confer a significant survival advantage, because the simultaneous presence of multiple variant genomes and the high rate of generation of new variants allows rapid selection of mutants better suited to new environmental conditions.[13]

Specific anti-HCV drugs that efficiently block virus production are not yet available. The current standard care is combination therapy with interferon (IFN)-α and the nucleoside analog ribavirin, which cures about 40% of hepatitis C patients infected by HCV genotype 1, the most prevalent genotype in industrialized countries, and about 80% of those infected by genotype 2 or 3.[14,15] Since many patients still do not benefit from the treatment and IFN therapy is associated with undesirable side effects such as headache, fever, severe depression, myalgia, arthralgia, and hemolytic anemia, development of innovative treatment alternatives for hepatitis C patients is immediately needed. Studies of HCV life cycle in cell cultures have been greatly facilitated by the development of genetically engineered viral genomes that are capable of self-amplifying to high levels (replicon system), and by recent establishment of a production system for recombinant infectious HCV. Such progress will aid in the development of significantly improved HCV antiviral agents.

Received: February 8, 2007 / Accepted: February 10, 2007
Reprint requests to: T. Suzuki

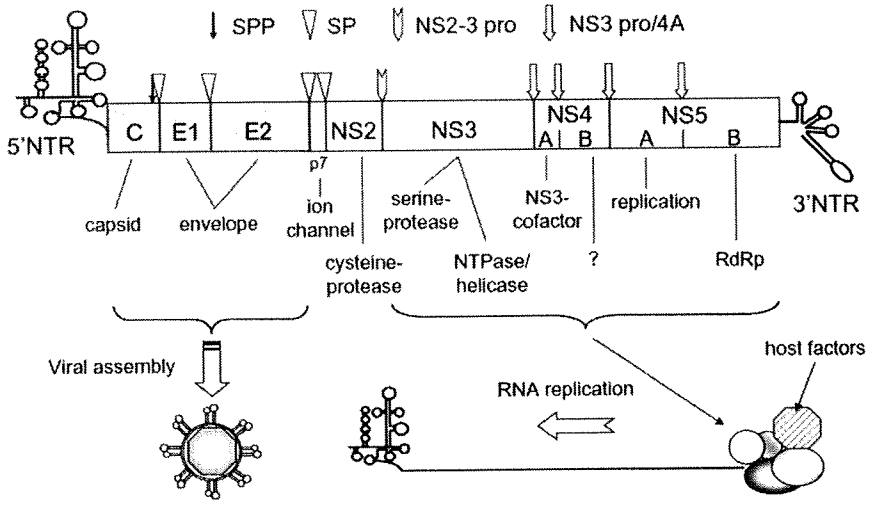

Fig. 1. Hepatitis C virus (HCV) genome organization and polyprotein processing. Posttranslational cleavages by signal peptide peptidase (*SPP*), signal peptidase (*SP*), NS2–NS3 protease (*NS2–3 pro*), and NS3 protease and NS4A complex (*NS3 pro/4A*) lead to the production of functional HCV proteins. *NTR*, nontranslated region

Cell culture systems for HCV research

Although substantial information on HCV protein structure and function has been obtained from the use of a variety of cell culture and in vitro expression systems, for many years, HCV research has been hampered by the restricted host range and the inefficiency of cell culture models for viral infection and propagation. The development of the HCV replicon system, therefore, is a milestone in HCV research and has allowed examination of viral RNA replication in cell culture.[16] Expression systems of heterologous virus genes based on RNA replicons have been established in a variety of positive-strand RNA viruses such as polio virus,[17–20] the alphavirus Semliki Forest virus,[21] Sindbis virus,[22–25] Kunjin virus,[26] human rhinovirus 14,[27] and bovine viral diarrhea virus.[28] In general, advantages of replicon systems are (1) a high level of gene expression and RNA replication, (2) easy construction of recombinants, and (3) a wide permissible host range.

The HCV replicons are typically composed of selectable, bicistronic RNA, with the first cistron containing the HCV 5′ nontranslated region (NTR), which directs translation of the gene encoding the neomycin phosphotransferase, and the second cistron containing the internal ribosome entry site (IRES) of the encephalomyocarditis virus, which directs translation of HCV NS3 through NS5B region, and the 3′ NTR. The prototype subgenomic replicon utilized a particular HCV genotype 1b clone termed Con1. Following transfection of RNA generated by in vitro transcription of the cloned replicon sequences into a human hepatoma cell line Huh-7, antibiotic G418-resistant cells could be obtained in which the subgenomic RNA replicated autonomously. RNA replication was first detected at relatively low frequency, followed by the identification of replicons harboring cell culture-adaptive mutations, which increased the efficiency of replication initiation by several orders of magnitude.[29–31]

Adaptive mutations were found primarily at the N-terminus of the NS3 helicase, in NS4B, and in the center of NS5A, which is upstream of the region putatively involved in IFN sensitivity. Most of the mutations in NS5A are located at highly conserved serine residues and lead to change in the phosphorylation state of NS5A.[32,33] A combination of adaptive mutation in NS3 and NS5A resulted in the highest level of replication of a particular HCV genotype 1b isolate.[31] Later work, however, has indicated that adaptive mutations can arise in most of the viral nonstructural proteins.[34,35] The mechanisms by which adaptive mutations increase RNA replication efficiency are not well understood.

In the last 7 years, a variety of different replicons have been generated, including replicons with reporters or markers such as luciferase and green fluorescent protein, replicons from genotype 1a and 2a, and genome-length dicistronic HCV RNAs (genomic HCV replicons). HCV replicons with reporter genes allow us to execute fast and reproducible screening of large series of compounds for antivirals.[36–38] Huh-7 cells are the most permissive for HCV replicons. However, variability in the permissiveness for replicons has been observed for a given Huh-7 cell pool, and the cells that are able to support efficient replication of the viral genome are enriched during selection such as G418 treatment. A so-called "cured" cell clone, which can be prepared by removing the replicons by treatment with IFN, supports viral replication to a much higher level in many cases and is useful for introducing genome-length HCV RNAs.[39,40]

An HCV genotype 2a replicon with the JFH-1 strain, which was first isolated from the serum of a Japanese patient with fulminant hepatitis C by our group,[41] replicates efficiently in not only Huh-7 cells but also other

hepatocyte-derived cell lines, HepG2 and IMY-N9, and nonhepatocyte-derived cell lines, HeLa and 293.[42-44] Interestingly, the JFH-1 replicon does not require adaptive mutations for replicating in these cell lines, and enormously efficient RNA replication is detected by transient replication assay as well as by colony formation assay with G418 selection,[42] suggesting that the JFH-1 genome can replicate autonomously without the help of drug selection or the requirement of adaptive mutations. This observation laid the basis for a breakthrough in HCV research.

Transfection of the full-length JFH-1 genome into Huh-7 cells leads to the production of HCV particles that are infectious both for naïve cells and for animal models.[45] As a first attempt, an in vitro transcribed full-length JFH-1 RNA was introduced into naïve Huh-7 cells, which is the original cell line used for subgenomic replicon studies. Efficient RNA replication in the transfected cells was detectable by Northern blot analysis, and the viral-enveloped particles, which are spherical structures with an outer diameter of approximately 55 nm, were secreted to the culture medium.[45] Secreted virus was found to be infectious, although at low efficiency, for naïve Huh-7 cells, and its infectivity can be neutralized by anti-CD81 antibody and hepatitis C patients' sera.[45] Subsequently, to increase the infection efficiency, "cured" Huh-7 cell lines such as Huh7.5, Huh7.5.1, and Huh7-Lunet were used. Infectivity of these cured cell lines with JFH-1 became more intense compared with standard Huh-7 cells, and the virus titers released from cells freshly transfected with the JFH-1 genome were markedly increased by continuous passage of the cells carrying persistent replicating viral RNA.[46] Further, chimeric constructs with the core to NS2 region of another genotype 2a clone, J6, improved the infectivity.[47] Thus, this recombinant infectious HCV cell culture system opens avenues of biochemical and genetic studies of the HCV life cycle.

Besides isolating functional molecular clones of HCV that replicate to high levels, to generate a cell culture model that mimics natural host cell environments may be advantageous for improving HCV production systems suitable for studying the virus–host interaction. It is likely that HCV morphogenesis occurs in a complex cellular environment in which host factors may either enhance or reduce the assembly and budding process. Generally, the interaction of viruses with polarized epithelia in the host is one of the key steps in the viral life cycle. A variety of enveloped viruses mature and bud from distinct membrane domains of the host cells.[48-51] We found that a dicistronic HCV genome of genotype 1b supports the production and secretion of infectious HCV particles in two independent three-dimensional (3D) culture systems, the radial-flow bioreactor (RFB) and the thermoreversible gelation polymer (TGP), but not in monolayer cultures, although its productivity is much lower than that observed in the JFH-1 system[52] (Fig. 2). The RFB system was initially aimed at the

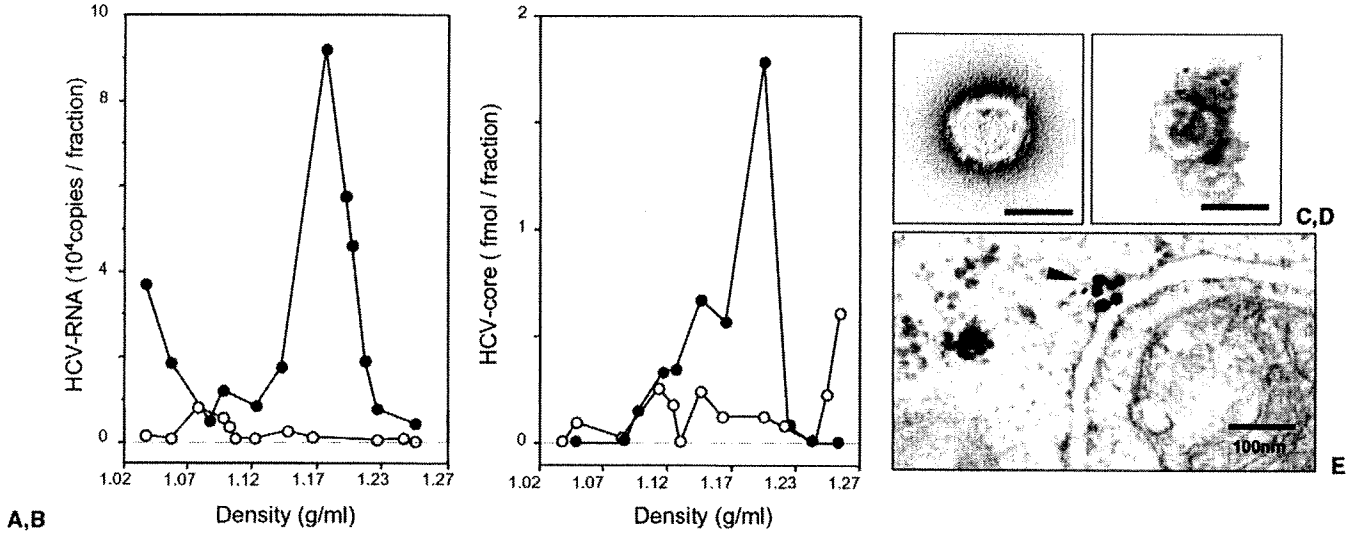

Fig. 2A–E. Production of HCV particles in the three-dimensional, thermoreversible gelatin polymer (TGP) culture of the Huh-7 cell line (RCYM1) carrying genome-length dicistronic HCV RNA of genotype 1b. **A, B** Sucrose density gradient analysis of culture supernatants of RCYM1 cells. The culture supernatants were fractionated and then HCV RNA (**A**) and core protein (**B**) in each fraction were determined by enzyme-linked immunosorbent assay and real-time reverse transcription polymerase chain reaction, respectively. *Closed circles*, TGP culture; *open circles*, monolayer culture. **C, D** Electron microscopy of HCV particles in the supernatants of TGP-cultured RCYM1 cells. **C** Negative staining. **D** Immunogold labeling with an anti-E2 antibody. Gold particles, 5 nm; bars, 50 nm. **E** Silver-intensified immunogold staining with anti-E1 antibody. The *arrowhead* indicates virus-like particles reacting with anti-E1 antibody

development of artificial liver tissue, and the bioreactor column consists of a vertically extended cylindrical matrix through which liquid medium flows continuously from the periphery toward the center of the reactor.[53] In RFB culture, human hepatocyte-derived cells can grow spherically or cubically, and they retain liver functions such as albumin synthesis[53–55] and drug-metabolizing activity mediated by cytochrome P450 3A4.[56] TGP is a chemically synthesized biocompatible polymer which has a sol–gel transition temperature, thus enabling us to culture cells three-dimensionally in the gel phase at 37°C and to harvest them in the sol phase at 4°C, without enzyme digestion.[57] In contrast to other matrix gels made from conventional natural polymers, TGP has several advantages that allow us to investigate the functional characteristics of epithelial cells, their tissue-like morphology, and their potential clinical applications. For example, the use of 3D culture materials other than TGP requires treatment with appropriate digestive enzymes or heating to collect cells grown as spheroids from the culture media, and the matrices may damage the cultured cells to some extent. A 3D culture system based on RFB and TGP, in which human hepatoma cells can assemble into spheroids with potentially polarized morphology, is a valuable tool in studies of HCV morphogenesis.

Translation

The approximately 341-nucleotide (nt)-long 5′ NTR is one of the most conserved regions of the HCV genome, and the secondary structural model, which is also largely conserved, reveals four distinct RNA domains in the region, reflecting its importance in both viral translation and replication.[58–61] The 5′ NTR forms four highly structured domains (domains I–IV), which may be conserved among HCV and related flaviviruses and pestiviruses,[59,60] and it is functionally characterized as an IRES to direct cap-independent translation of the genome.[62,63] To determine the minimal sequence required for HCV IRES-dependent translation, as in the earlier studies of picornaviruses, the bicistronic RNAs in which two reporter protein-coding sequences are separated by an IRES sequence were analyzed. Translation of the upstream reading frame occurs in a 5′ end-dependent fashion, while translation of the downstream reading frame is driven by the IRES element. The IRES comprises nearly the entire 5′ UTR of the genome. There is evidence to suggest that the first 12 to 30 nt of the coding sequence are also important for IRES activity.[64–66] The first 40 nt of the 5′ NTR, which includes a single stem–loop (domain I), is not essential for the translation; the 5′ border of the IRES was mapped between nt 38 and 46.[61,67,68] Domains II and III are relatively more complex and contain multiple stems and loops.[60,69] Domain IV consists of a small stem–loop containing the polyprotein start codon at nt 342 and forms a pseudoknot via base-pairing with a loop in domain III.

Recruitment of the 43S ribosomal complex, containing a small 40S ribosomal subunit, eukaryotic initiation factor (eIF) 3, and a tRNA–eIF2–GTP ternary complex, to mRNA molecules is critical for initiation of eukaryotic protein synthesis. The 40S subunit and eIF3 can bind independently to the HCV IRES.[64,70–72] However, it appears that interaction between IRES RNA and the 40S subunit drives formation of an IRES–40S subunit–eIF3 complex, since HCV IRES RNA demonstrates similar affinity to both the 40S subunit and the 40S–eIF complex.[71] Other cellular factors such as La autoantigen,[73–75] heterogeneous ribonucleoprotein L,[76] poly-C binding protein,[77,78] and pyrimidine tract-binding protein,[79,80] also bind to the IRES element and modulate translation.

Regulation of IRES-dependent translation of HCV is also likely to involve viral factors. We found that the core protein specifically inhibits HCV translation, possibly by binding to a stem–loop IIId domain, particularly a GGG triplet within the hairpin loop structure of the domain, within the IRES (Fig. 3).[79–81] Although a conflicting report has suggested that inhibition of HCV translation is due to an RNA–RNA interaction, rather than to an interaction between RNA and the core protein,[82] later studies support the role of a core protein sequence spanning amino acids (aa) 34–44 in inhibition of viral translation through its interaction with the IRES.[83] Furthermore, the N-terminal 20 residues of the core protein have been shown to selectively inhibit translation mediated by HCV IRES in a cell type-specific manner.[84] We propose a model in which competitive binding of the core protein to the IRES and 40S ribosomal subunit regulates HCV translation.

By analogy with other RNA viruses with IRES-mediated expression, the HCV 5′ NTR has been expected to contain not only determinants for translation but also *cis*-acting elements for RNA replication. Recent studies demonstrated that (1) the sequence upstream of the IRES is essential for viral RNA replication, (2) sequences within the IRES are required for high-level HCV replication, and (3) the stem–loop domain II of the IRES is crucial for the replication.[85]

Polyprotein processing

IRES-mediated translation of the HCV ORF yields a polyprotein precursor that is subsequently processed by cellular and viral proteases into mature structural and nonstructural proteins (Fig. 1). As deduced from the hydrophobicity profile and the dependence on micro-

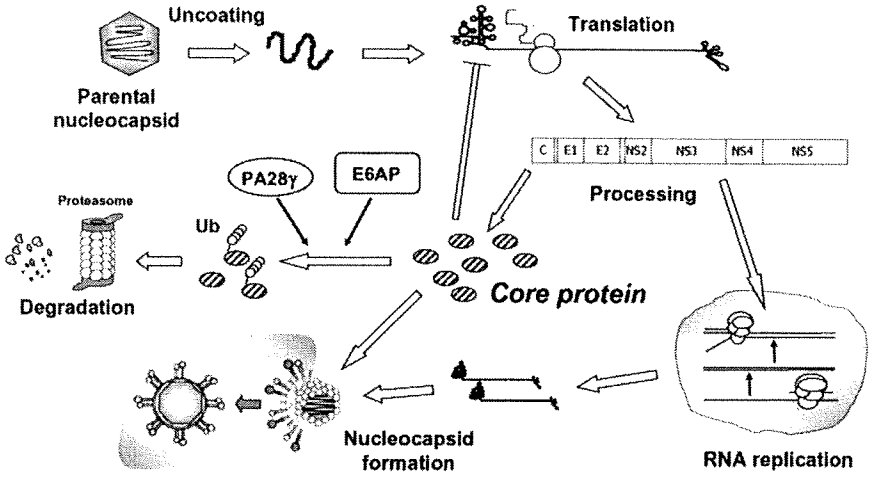

Fig. 3. The role and fate of HCV core protein in the postulated HCV life cycle. See text for further explanation and details

somal membranes, junctions at core/E1, E1/E2, E2/p7, and p7/NS2 are processed by host signal peptidases. For instance, secondary structure analysis of the core protein reveals that all major alpha helices are located in the C-terminal half of the protein. A predicted alpha helix encoded by aa 174–191 is extremely hydrophobic and resembles typical signal peptide sequences. Further posttranslational cleavage close to the C terminus of the core protein takes place, removing the E1 signal sequence by the signal peptide peptidase.[86–89] This peptidase has recently been identified[90] and exhibits protease activity within cellular membranes, resulting in cleavage of peptide bonds in the plane of lipid bilayers.

The viral nonstructural proteins are processed by two viral proteases: processing between NS2 and NS3 is a rapid intramolecular reaction that is accomplished by the NS2–3 protease, which spans NS2 and the N-terminal domain of NS3, whereas the remaining four junctions are cleaved by the serine protease located at the N-terminal 180 residues of NS3 protein. Efficient cleavage at the NS2/3 site requires the 130 C-terminal residues and the first 180 aa of NS3. Recombinant proteins lacking the N-terminal membrane domain of NS2 were found to be enzymatically active, allowing further characterization of this activity.[91,92] Deletion of NS2 from the nonstructural polyprotein did not abolish the replication of HCV RNA in cell cultures, indicating that NS2 is not essential for vial RNA replication.[16,29]

The NS3–NS5B region is processed presumably with the following preferred order of cleavage: NS3/4A→NS5A/5B→NS4A/4B→NS4B/5A.[93–96] Processing at the NS3/4A site is an intramolecular reaction, whereas cleavage at the other sites can be mediated intermolecularly. NS3 is a multifunctional molecule. Besides its N-terminal protease activity, the helicase and nucleotide triphosphatase (NTPase) activities reside in the C-terminal 500 residues of the NS3 protein.[97–101] NS4A functions as a cofactor of the NS3 serine protease and is required for efficient polyprotein processing. There are significant differences in the stability and activity of the NS3 protease in the presence or absence of NS4A. NS3 protein is relatively unstable when expressed in cells in the absence of NS4A.[102] Structural studies by nuclear magnetic resonance and X-ray methods show that the NS3–4A complex has a more highly ordered N-terminal domain and NS4A binding leads the NS3 protease to a rearrangement of the active site triad to a canonical conformation.[103] It has been predicted that the N-terminus of NS4A forms a transmembrane helix, which presumably anchors the NS3–4A complex to the cellular membrane.[104]

RNA replication

HCV is assumed to replicate its genome through the synthesis of a full-length negative-strand RNA. Positive-strand RNA is then produced from the negative-strand template; it is several-fold more abundant than the negative-stranded RNA and is utilized for translation, replication, and packaging into progeny viruses. RNA replication of most RNA viruses involves certain intracellular membrane structures, including the endoplasmic reticulum (ER),[105–107] Golgi,[108] endosomes, and lysosomes.[109] HCV RNA replication is also believed to occur in the cytoplasm of the virus-infected cells.

Although NS5B protein has RNA-dependent RNA polymerase (RdRp) activity in vitro, its recombinant product alone is presumably short of strict template specificity and fidelity, which are essential for viral RNA synthesis. It is highly likely that other viral or host factors are important for conferring proper RNA replication and that the replication complexes (RCs), which are composed of NS5B and additional components re-

quired for modulating polymerase activity, are involved in catalyzing HCV RNA synthesis during the replication process. NS3 is directly involved in RNA synthesis, possibly through its helicase/NTPase activities. The helicase activity is presumed to be involved in unwinding a putative double-stranded replication intermediate or to remove regions of secondary structure so that MS5B RdRp can copy both strands of the viral RNA. It is likely that the NTPase activity is coupled with the helicase function, supplying the energy required for disrupting RNA duplexes. Although little is known about the function of NS4B in the HCV life cycle to date, NS4B protein can induce a membranous web, consisting of small vesicles embedded in a membranous matrix,[110] and it has been reported that the newly synthesized HCV RNA and most of the viral nonstructural proteins occur in these membrane webs or speckle-like structures.[111–113] NS4B may play an important role in the formation of the HCV RNA replication complex.[114] Evidence indicating an involvement of NS5A in viral RNA replication is now accumulating. As described above, a hot spot of the cell culture-adaptive mutations that increase replication efficiency of HCV RNA is located in the central region of NS5A.[29–31] The membrane association of NS5A through its amino-terminal transmembrane domain[115] and the interaction between NS5A and 5B[116] are essential for RNA replication. Several cellular proteins interacting with NS5A have been identified, and human vesicle-associated membrane protein-associated proteins (hVAP-A and -B) are likely to play a key role in RNA replication through the interaction with NS5A.[114,117] The 3′ NTR also contains a significant predicted RNA structure with three distinct domains: a variable region of about 40 nt, a variable length poly(U/UC) tract, and a highly conserved, 98-nt 3′ terminal segment (3′X) that putatively forms three stem–loop structures.[118–120] Viral RNA replication was not detected when any of the three putative stem–loop structures within the 3′X region or the entire poly(U/UC) was deleted.[121] The variable region segment also contributes to efficient RNA replication.[122]

Several groups have succeeded in demonstrating the in vitro replication activities of HCV RCs in crude membrane fractions of cells harboring the subgenomic replicons.[123–126] These cell-free systems provide a valuable complement to the in vitro RdRp assays for biochemical dissection of HCV RNA replication and are a useful source for isolation of viral RCs. From the in vitro replication studies, it appears that RNA synthesis can be initiated in the absence of added negative-strand template RNA, suggesting that preinitiated template RNA copurifies with the RC.[124,125,127] Although the newly synthesized single-strand RNA can be used as a template for a further round of double-strand RNA synthesis, no exogenous RNA serves as a template for HCV RC preparation.[125] Added RNA templates might not access the active site of the HCV RCs owing to sequestration by membranes. The HCV RCs contain both positive- and negative-strand RNAs.[124,127] It has also been reported that cell-free replication activity increases at temperatures ranging from 25° to 40°C, and divalent cations (Mn^{2+} and Mg^{2+}) can be used in the reaction.[125,127]

Membrane flotation analysis and a replication assay have shown that viral RNA and proteins are present in detergent-resistant membrane structures, most likely a lipid-raft structure, and RNA replication activity was detected even after treatment with detergent.[123,128] Lipid rafts are cholesterol- and sphingolipid–rich microdomains characterized by detergent insolubility.[129–131] These structures are known to play a critical role in a number of biological processes, such as as regulators and organizing centers of signal transduction and membrane traffic pathways, including virus entry and assembly of, for example, influenza virus,[132–134] human immunodeficiency virus type-1,[27,135,136] Ebola virus, Marburg virus,[137] enterovirus,[138] avian sarcoma and leukosis virus,[139] Coxsackie B virus, adenovirus,[140] measles virus,[16] and respiratory syncytial virus.[141] However, HCV may be the first example of the association of a lipid raft with viral RNA replication.

On the other hand, it has been widely believed that most of the HCV life cycle, including protein processing and genome replication, takes place in the ER, where cholesterol–sphingolipid rafts are not assembled.[110,142–144] Several studies using the replicon system have indicated that the nonstructural proteins are associated with the ER.[143,145] Nevertheless, it is still possible that HCV nonstructural proteins synthesized at the ER relocalize to lipid-raft membranes when they are actively engaged in RNA replication. It has been shown by membrane separation analysis that HCV nonstructural proteins are present both in the ER and the Golgi, but the activity of viral RNA replication was detected mainly in the Golgi fraction.[123,146] Further studies to elucidate where and how the HCV genome replicates in infected cells are needed.

Viral assembly

The assembly of HCV and the virion structure remains largely unknown. By analogy with related viruses, the mature HCV virion presumably possesses a nucleocapsid and outer envelope composed of a lipid membrane and envelope proteins. HCV virions are thought to have a diameter of 40–70 nm.[147,148] These observations were recently confirmed by immunoelectron microscopy of infectious HCV particles produced in cell cultures.[45,52] It has been reported that HCV circulates in various forms

in the sera of infected hosts, for example, as (1) free mature virions, (2) virions bound to low-density lipoproteins and very low density lipoproteins, (3) virions bound to immunoglobulins, and (4) nonenveloped nucleocapsids, which exhibit physicochemical and antigenic properties.[147-150]

The HCV structural proteins (core, E1, and E2) are located in the N-terminal one-third of the precursor polyprotein (Fig. 1). A crucial function of the core protein, which is derived from the N-terminus of the viral polyprotein, is assembly of the viral nucleocapsid. The aa sequence of this protein is well conserved among different HCV strains, compared with other HCV proteins. The N-terminal domain of the core protein is highly basic, while its C-terminus is hydrophobic. When expressed in mammalian cells and transgenic mice, the core protein is found on membranes of the ER, on the surface of lipid droplets, on the mitochondrial outer membrane, and, to some extent, in the nucleus.[151-156] The core protein is likely multifunctional and is not only involved in formation of the HCV virion but also has a number of regulatory functions, including modulation of lipid metabolism and hepatocarcinogenesis.[153,157-159] The envelope proteins E1 and E2 are extensively glycosylated and have an apparent molecular weight of 30–35 and 70–75 kDa, respectively. Predictive algorithms and genetic analyses of deletion mutants and glycosylation-site variants of the E1 protein suggest that E1 can adopt two topologies in the ER membrane: the conventional type I membrane topology and a polytopic topology in which the protein spans the ER membrane twice with an intervening cytoplasmic loop.[160] E1 and E2 proteins form a noncovalent complex, which is believed to be the building block of the viral envelope.

Several expression systems have been used to investigate HCV capsid assembly using mammalian, insect, yeast, bacteria, and reticulocyte lysates, as well as purified recombinant proteins.[148,161-170] The results suggest that immunogenic nucleocapsid-like particles are heterologous in size and range from 30 to 80 nm in diameter. The N-terminal half of the core protein is important for nucleocapsid formation.[163,169,170] HCV capsid formation occurs in the presence or absence of ER-derived membrane, which supports cleavage of the signal peptide at the C-terminus.[170]

Nucleocapsid assembly generally involves oligomerization of the capsid protein and encapsidation of genomic RNA. In fact, study of a recombinant mature core protein has shown it to exist as a large multimer in solution under physiological conditions, within which stable secondary structures have been observed.[171] Studies using yeast two-hybrid systems have identified a potential homotypic interaction domain within the N-terminal region of the core protein (aa 1–115 or –122), with particular emphasis on the region encompassing aa 82–102.[172,173] However, other studies have identified two C-terminal regions, extending from aa 123 to 191 and from 125 to 179, as responsible for self-interaction. Furthermore, Pro substitution within these C-terminal regions has been observed to abolish core protein self-interaction.[171,174] Circular dichroism spectroscopy has further shown that a Trp-rich region spanning aa 76–113 is largely solvent-exposed and unlikely to play a role in multimerization.[171] Recently, our group demonstrated that self-oligomerization of the core protein is promoted by aa 72–91 in the core.[160]

Once a HCV nucleocapsid is formed in the cytoplasm, it acquires an envelope as it buds through intracellular membranes. Interactions between the core and E1/E2 proteins are considered to determine viral morphology. Expression of HCV structural proteins using recombinant virus vectors has led to successful generation of virus-like particles with similar ultrastructural properties to HCV virions. Packaging of these HCV-like particles into intracellular vesicles as a result of budding from the ER has been noted.[161,175,176] Mapping studies to determine the nature of interaction between core and E1 proteins have demonstrated the importance of C-terminal regions in this interaction.[177,178] Since corresponding sequences are not well conserved among various HCV isolates, interactions between core and E1 proteins might depend more on hydrophobicity than on specific sequences. By contrast, it has been shown that interaction between the self-oligomerized HCV core and the E1 glycoprotein is mediated through the cytoplasmic loop present in a polytopic form of the E1 protein.[160]

Implication of the ubiquitin–proteasome pathway in core protein maturation

The ubiquitin–proteasome pathway is the major route by which selective protein degradation occurs in eukaryotic cells and is now emerging as an essential mechanism of cellular regulation.[179,180] This pathway is also involved in the posttranslational regulation of the core protein.[158,181-183] We have reported that processing at the carboxyl-terminal hydrophobic domain of the core protein leads to its efficient polyubiquitylation and proteasomal degradation.[181] Recently, our group identified the ubiquitin ligase E6AP as an HCV core-binding protein and showed that E6AP enhances ubiquitylation and degradation of the mature as well as the carboxyl-terminally truncated core proteins, and that the core protein produced from infectious HCV is degraded via an E6AP-dependent pathway (Fig. 3).[183] E6AP, the prototype of HECT domain ubiquitin ligases,[184] was initially identified as the cellular factor that stimulates ubiquitin-dependent degradation of the tumor suppres-

sor p53 in conjunction with E6 protein of cancer-associated human papillomavirus types 16 and 18.[185,186] Exogenous expression of E6AP reduces intracellular core protein levels and supernatant viral infectivity in infected cell cultures. Knockdown of exogenous E6AP by siRNA increases intracellular core protein levels and virus titers in the culture supernatants. The core protein interacts with E6AP through the aa 58–71 region of the core, which is highly conserved among all HCV genotypes, suggesting that E6AP-dependent degradation of the core protein is common to a variety of HCV isolates and plays a critical role in the HCV life cycle or viral pathogenesis.

A role for the proteasome activator PA28γ core-binding protein in degradation of the core protein has also been demonstrated (Fig. 3).[158,182] Overexpression of PA28γ promotes proteolysis of the core protein. PA28γ predominates in the nucleus and forms a homopolymer, which associates with the 20S proteasome,[187] thereby enhancing proteasomal activity.[188] Both nuclear retention and core protein stability are regulated via a PA28γ-dependent pathway.

In eukaryotic cells, targeted protein degradation is increasingly understood to be an important mechanism by which cells regulate levels of specific proteins, and thereby regulate their function. The core protein is believed to play a key role in viral replication and pathogenesis since it forms the viral particle and regulates a number of host cell functions. Although the biological significance of ubiquitylation and proteasomal degradation of the core protein is not fully understood, E6AP possibly affects the production of HCV particles through controlling the amount of core protein (Fig. 3). This mechanism may contribute to virus persistence by maintaining a (moderately) low level of the viral nucleocapsid. The E6AP binding domain within the core protein resides in the region that is considered to be important for binding to the viral RNA and several host factors.[189] These factors may affect the interaction between the core and E6AP, resulting in control of E6AP-dependent core degradation. A recent study demonstrated that a knockdown of the *PA28γ* gene induces the accumulation of the core protein in the nucleus of hepatocytes of HCV core gene-transgenic mice and disrupts development of both hepatic steatosis and hepatocellular carcinoma.[158] Upregulation of several genes related to fatty acid biosynthesis and lipid homeostasis by the core protein was observed in the cells and the mouse liver in the PA28γ-dependent manner. Thus, it is likely that PA28γ plays an important role in the development of liver pathology induced by HCV infection.

Acknowledgments. The authors are grateful to all their coworkers who contributed to the studies cited here, most especially Tatsuo Miyamura. We also thank T. Mizoguchi for secretarial work. This work was supported in part by a grant for Research on Health Sciences focusing on Drug Innovation from the Japan Health Sciences Foundation; and by Grants-in-Aid from the Ministry of Health, Labour and Welfare, Japan.

References

1. Kuo G, Choo QL, Alter HJ, Gitnick GL, Redeker AG, Purcell RH, et al. An assay for circulating antibodies to a major etiologic virus of human non-A, non-B hepatitis. Science 1989;244:362–4.
2. Grakoui A, Hanson HL, Rice CM. Bad time for Bonzo? Experimental models of hepatitis C virus infection, replication, and pathogenesis. Hepatology 2001;33:489–95.
3. Lauer GM, Walker BD. Hepatitis C virus infection. N Engl J Med 2001;345:41–52.
4. Saito I, Miyamura T, Ohbayashi A, Harada H, Katayama T, Kikuchi S, et al. Hepatitis C virus infection is associated with the development of hepatocellular carcinoma. Proc Natl Acad Sci USA 1990;87:6547–9.
5. Alter MJ. Epidemiology of hepatitis C in the West. Semin Liver Dis 1995;15:5–14.
6. Di Bisceglie AM. Hepatitis C and hepatocellular carcinoma. Hepatology 1997;26:34S–8S.
7. Poynard T, Yuen MF, Ratziu V, Lai CL. Viral hepatitis C. Lancet 2003;362:2095–100.
8. Pawlotsky JM. Pathophysiology of hepatitis C virus infection and related liver disease. Trends Microbiol 2004;12:96–102.
9. Houghton M, Weiner A, Han J, Kuo G, Choo Q-L. Molecular biology of the hepatitis C viruses: implications for diagnosis, development and control of viral disease. Hepatology 1991;14:381–8.
10. Robertson B, Myers G, Howard C, Brettin T, Bukh J, Gaschen B, et al. Classification, nomenclature, and database development for hepatitis C virus (HCV) and related viruses: proposals for standardization. International Committee on Virus Taxonomy. Arch Virol 1998;143:2493–503.
11. Choo QL, Kuo G, Weiner AJ, Overby LR, Bradley DW, Houghton M. Isolation of a cDNA clone derived from a blood-borne non-A, non-B viral hepatitis genome. Science 1989;244:359–62.
12. Martell M, Esteban JI, Quer J, Genesca J, Weiner A, Esteban R, et al. Hepatitis C virus (HCV) circulates as a population of different but closely related genomes: quasispecies nature of HCV genome distribution. J Virol 1992;66:3225–9.
13. Pawlotsky JM. Hepatitis C virus population dynamics during infection. Curr Top Microbiol Immunol 2006;299:261–84.
14. Zeuzem S, Feinman SV, Rasenack J, Heathcote EJ, Lai MY, Gane E, et al. Peginterferon alpha-2a in patients with chronic hepatitis C. N Engl J Med 2000;343:1666–72.
15. Heathcote EJ, Shiffman ML, Cooksley WG, Dusheiko GM, Lee SS, Balart L, et al. Peginterferon alpha-2a in patients with chronic hepatitis C and cirrhosis. N Engl J Med 2000;343:1673–80.
16. Lohmann V, Korner F, Koch J, Herian U, Theilmann L, Bartenschlager R. Replication of subgenomic hepatitis C virus RNAs in a hepatoma cell line. Science 1999;285:110–3.
17. Andino R, Rieckhof GE, Achacoso PL, Baltimore D. Poliovirus RNA synthesis utilizes an RNP complex formed around the 5′-end of viral RNA. EMBO J 1993;12:3587–98.
18. Collis PS, O'Donnell BJ, Barton DJ, Rogers JA, Flanegan JB. Replication of poliovirus RNA and subgenomic RNA transcripts in transfected cells. J Virol 1992;66:6480–8.
19. Hagino-Yamagishi K, Nomoto A. In vitro construction of poliovirus defective interfering particles. J Virol 1989;63:5386–92.

20. Kaplan G, Racaniello VR. Construction and characterization of poliovirus subgenomic replicons. J Virol 1988;62:1687–96.
21. Liljestrom P, Garoff H. A new generation of animal cell expression vectors based on the Semliki Forest virus replicon. Biotechnology (NY) 1991;9:1356–61.
22. Bredenbeek PJ, Frolov I, Rice CM, Schlesinger S. Sindbis virus expression vectors: packaging of RNA replicons by using defective helper RNAs. J Virol 1993;67:6439–46.
23. Johanning FW, Conry RM, LoBuglio AF, Wright M, Sumerel LA, Pike MJ, et al. A Sindbis virus mRNA polynucleotide vector achieves prolonged and high level heterologous gene expression in vivo. Nucleic Acids Res 1995;23:1495–501.
24. Kamrud KI, Powers AM, Higgs S, Olson KE, Blair CD, Carlson JO, et al. The expression of chloramphenicol acetyltransferase in mosquitoes and mosquito cells using a packaged Sindbis replicon system. Exp Parasitol 1995;81:394–403.
25. Xiong C, Levis R, Shen P, Schlesinger S, Rice CM, Huang HV. Sindbis virus: an efficient, broad host range vector for gene expression in animal cells. Science 1989;243:1188–91.
26. Khromykh AA, Westaway EG. Subgenomic replicons of the flavivirus Kunjin: construction and applications. J Virol 1997;71:1497–505.
27. McKnight KL, Lemon SM. Capsid coding sequence is required for efficient replication of human rhinovirus 14 RNA. J Virol 1996;70:1941–52.
28. Behrens SE, Grassmann CW, Thiel HJ, Meyers G, Tautz N. Characterization of an autonomous subgenomic pestivirus RNA replicon. J Virol 1998;72:2364–72.
29. Blight KJ, Kolykhalov AA, Rice CM. Efficient initiation of HCV RNA replication in cell culture. Science 2000;290:1972–4.
30. Krieger N, Lohmann V, Bartenschlager R. Enhancement of hepatitis C virus RNA replication by cell culture-adaptive mutations. J Virol 2001;75:4614–24.
31. Lohmann V, Korner F, Dobierzewska A, Bartenschlager R. Mutations in hepatitis C virus RNAs conferring cell culture adaptation. J Virol 2001;75:1437–49.
32. Evans MJ, Rice CM, Goff SP. Phosphorylation of hepatitis C virus nonstructural protein 5A modulates its protein interactions and viral RNA replication. Proc Natl Acad Sci USA 2004;101:13038–43.
33. Appel N, Pietschmann T, Bartenschlager R. Mutational analysis of hepatitis C virus nonstructural protein 5A: potential role of differential phosphorylation in RNA replication and identification of a genetically flexible domain. J Virol 2005;79:3187–94.
34. Lohmann V, Hoffmann S, Herian U, Penin F, Bartenschlager R. Viral and cellular determinants of hepatitis C virus RNA replication in cell culture. J Virol 2003;77:3007–19.
35. Yi M, Lemon SM. Adaptive mutations producing efficient replication of genotype 1a hepatitis C virus RNA in normal Huh7 cells. J Virol 2004;78:7904–15.
36. Bartenschlager R. Hepatitis C virus molecular clones: from cDNA to infectious virus particles in cell culture. Curr Opin Microbiol 2006;9:416–22.
37. Brass V, Moradpour D, Blum HE. Molecular virology of hepatitis C virus (HCV): 2006 update. Int J Med Sci 2006;3:29–34.
38. Bartenschlager R. The hepatitis C virus replicon system: from basic research to clinical application. J Hepatol 2005;43:210–6.
39. Blight KJ, McKeating JA, Rice CM. Highly permissive cell lines for subgenomic and genomic hepatitis C virus RNA replication. J Virol 2002;76:13001–14.
40. Friebe P, Boudet J, Simorre JP, Bartenschlager R. Kissing-loop interaction in the 3′ end of the hepatitis C virus genome essential for RNA replication. J Virol 2005;79:380–92.
41. Kato T, Furusaka A, Miyamoto M, Date T, Yasui K, Hiramoto J, et al. Sequence analysis of hepatitis C virus isolated from a fulminant hepatitis patient. J Med Virol 2001;64:334–9.
42. Kato T, Date T, Miyamoto M, Furusaka A, Tokushige K, Mizokami M, et al. Efficient replication of the genotype 2a hepatitis C virus subgenomic replicon. Gastroenterology 2003;125:1808–17.
43. Date T, Kato T, Miyamoto M, Zhao Z, Yasui K, Mizokami M, et al. Genotype 2a hepatitis C virus subgenomic replicon can replicate in HepG2 and IMY-N9 cells. J Biol Chem 2004;279:22371–6.
44. Kato T, Date T, Miyamoto M, Zhao Z, Mizokami M, Wakita T. Nonhepatic cell lines HeLa and 293 support efficient replication of the hepatitis C virus genotype 2a subgenomic replicon. J Virol 2005;79:592–6.
45. Wakita T, Pietschmann T, Kato T, Date T, Miyamoto M, Zhao Z, et al. Production of infectious hepatitis C virus in tissue culture from a cloned viral genome. Nat Med 2005;11:791–6.
46. Zhong J, Gastaminza P, Cheng G, Kapadia S, Kato T, Burton DR, et al. Robust hepatitis C virus infection in vitro. Proc Natl Acad Sci USA 2005;102:9294–9.
47. Lindenbach BD, Evans MJ, Syder AJ, Wolk B, Tellinghuisen TL, Liu CC, et al. Complete replication of hepatitis C virus in cell culture. Science 2005;309:623–6.
48. Compans RW. Virus entry and release in polarized epithelial cells. Curr Top Microbiol Immunol 1995;202:209–19.
49. Garoff H, Hewson R, Opstelten DJ. Virus maturation by budding. Microbiol Mol Biol Rev 1998;62:1171–90.
50. Schmitt AP, Lamb RA. Escaping from the cell: assembly and budding of negative-strand RNA viruses. Curr Top Microbiol Immunol 2004;283:145–96.
51. Takimoto T, Portner A. Molecular mechanism of paramyxovirus budding. Virus Res 2004;106:133–45.
52. Murakami K, Ishii K, Ishihara Y, Yoshizaki S, Tanaka K, Gotoh Y, et al. Production of infectious hepatitis C virus particles in three-dimensional cultures of the cell line carrying the genome-length dicistronic viral RNA of genotype 1b. Virology 2006;351:381–92.
53. Kawada M, Nagamori S, Aizaki H, Fukaya K, Niiya M, Matsuura T, et al. Massive culture of human liver cancer cells in a newly developed radial flow bioreactor system: ultrafine structure of functionally enhanced hepatocarcinoma cell lines. In Vitro Cell Dev Biol Anim 1998;34:109–15.
54. Matsuura T, Kawada M, Hasumura S, Nagamori S, Obata T, Yamaguchi M, et al. High density culture of immortalized liver endothelial cells in the radial-flow bioreactor in the development of an artificial liver. Int J Artif Organs 1998;21:229–34.
55. Aizaki H, Nagamori S, Matsuda M, Kawakami H, Hashimoto O, Ishiko H, et al. Production and release of infectious hepatitis C virus from human liver cell cultures in the three-dimensional radial-flow bioreactor. Virology 2003;314:16–25.
56. Iwahori T, Matsuura T, Maehashi H, Sugo K, Saito M, Hosokawa M, et al. CYP3A4 inducible model for in vitro analysis of human drug metabolism using a bioartificial liver. Hepatology 2003;37:665–73.
57. Yoshioka H, Mikami M, Mori Y, Tsuchida E. A synthetic hydrogel with thermoreversible gelation. J Macromol Sci 1994;A31:113–20.
58. Bukh J, Purcell RH, Miller RH. Sequence analysis of the 5′ noncoding region of hepatitis C virus. Proc Natl Acad Sci USA 1992;89:4942–6.
59. Brown EA, Zhang H, Ping LH, Lemon SM. Secondary structure of the 5′ nontranslated regions of hepatitis C virus and pestivirus genomic RNAs. Nucleic Acids Res 1992;20:5041–5.
60. Honda M, Beard MR, Ping LH, Lemon SM. A phylogenetically conserved stem–loop structure at the 5′ border of the internal ribosome entry site of hepatitis C virus is required for cap-independent viral translation. J Virol 1999;73:1165–74.
61. Honda M, Brown EA, Lemon SM. Stability of a stem–loop involving the initiator AUG controls the efficiency of internal initiation of translation on hepatitis C virus RNA. RNA 1996;2:955–68.

62. Tsukiyama-Kohara K, Iizuka N, Kohara M, Nomoto A. Internal ribosome entry site within hepatitis C virus RNA. J Virol 1992; 66:1476–83.
63. Wang C, Sarnow P, Siddiqui A. Translation of human hepatitis C virus RNA in cultured cells is mediated by an internal ribosome-binding mechanism. J Virol 1993;67:3338–44.
64. Hellen CU, Pestova TV. Translation of hepatitis C virus RNA. J Viral Hepat 1999;6:79–87.
65. Lu HH, Wimmer E. Poliovirus chimeras replicating under the translational control of genetic elements of hepatitis C virus reveal unusual properties of the internal ribosomal entry site of hepatitis C virus. Proc Natl Acad Sci USA 1996;93:1412–7.
66. Reynolds JE, Kaminski A, Kettinen HJ, Grace K, Clarke BE, Carroll AR, et al. Unique features of internal initiation of hepatitis C virus RNA translation. EMBO J 1995;14:6010–20.
67. Rijnbrand R, Bredenbeek P, van der Straaten T, Whetter L, Inchauspe G, Lemon S, et al. Almost the entire 5′ non-translated region of hepatitis C virus is required for cap-independent translation. FEBS Lett 1995;365:115–9.
68. Yoo BJ, Spaete RR, Geballe AP, Selby M, Houghton M, Han JH. 5′ end-dependent translation initiation of hepatitis C viral RNA and the presence of putative positive and negative translational control elements within the 5′ untranslated region. Virology 1992;191:889–99.
69. Lemon S, Honda M. Internal ribosome entry sites within the RNA genomes of hepatitis C virus and other flaviviruses. Semin Virol 1997;8:274–88.
70. Buratti E, Tisminetzky S, Zotti M, Baralle FE. Functional analysis of the interaction between HCV 5′UTR and putative subunits of eukaryotic translation initiation factor eIF3. Nucleic Acids Res 1998;26:3179–87.
71. Kieft JS, Zhou K, Jubin R, Doudna JA. Mechanism of ribosome recruitment by hepatitis C IRES RNA. RNA 2001;7:194–206.
72. Sizova DV, Kolupaeva VG, Pestova TV, Shatsky IN, Hellen CU. Specific interaction of eukaryotic translation initiation factor 3 with the 5′ nontranslated regions of hepatitis C virus and classical swine fever virus RNAs. J Virol 1998;72:4775–82.
73. Ali N, Pruijn GJ, Kenan DJ, Keene JD, Siddiqui A. Human La antigen is required for the hepatitis C virus internal ribosome entry site-mediated translation. J Biol Chem 2000;275:27531–40.
74. Ali N, Siddiqui A. The La antigen binds 5′ noncoding region of the hepatitis C virus RNA in the context of the initiator AUG codon and stimulates internal ribosome entry site-mediated translation. Proc Natl Acad Sci USA 1997;94:2249–54.
75. Isoyama T, Kamoshita N, Yasui K, Iwai A, Shiroki K, Toyoda H, et al. Lower concentration of La protein required for internal ribosome entry on hepatitis C virus RNA than on poliovirus RNA. J Gen Virol 1999;80:2319–27.
76. Hahm B, Kim YK, Kim JH, Kim TY, Jang SK. Heterogeneous nuclear ribonucleoprotein L interacts with the 3′ border of the internal ribosomal entry site of hepatitis C virus. J Virol 1998; 72:8782–8.
77. Fukushi S, Okada M, Kageyama T, Hoshino FB, Nagai K, Katayama K. Interaction of poly(rC)-binding protein 2 with the 5′-terminal stem loop of the hepatitis C-virus genome. Virus Res 2001;73:67–79.
78. Anwar A, Ali N, Tanveer R, Siddiqui A. Demonstration of functional requirement of polypyrimidine tract-binding protein by SELEX RNA during hepatitis C virus internal ribosome entry site-mediated translation initiation. J Biol Chem 2000;275: 34231–5.
79. Shimoike T, Mimori S, Tani H, Matsuura Y, Miyamura T. Interaction of hepatitis C virus core protein with viral sense RNA and suppression of its translation. J Virol 1999;73:9718–25.
80. Tanaka Y, Shimoike T, Ishii K, Suzuki R, Suzuki T, Ushijima H, et al. Selective binding of hepatitis C virus core protein to synthetic oligonucleotides corresponding to the 5′ untranslated region of the viral genome. Virology 2000;270:229–36.
81. Shimoike T, Koyama C, Murakami K, Suzuki R, Matsuura Y, Miyamura T, et al. Down-regulation of the internal ribosome entry site (IRES)-mediated translation of the hepatitis C virus: critical role of binding of the stem–loop IIId domain of IRES and the viral core protein. Virology 2006;345:434–45.
82. Wang TH, Rijnbrand RC, Lemon SM. Core protein-coding sequence, but not core protein, modulates the efficiency of cap-independent translation directed by the internal ribosome entry site of hepatitis C virus. J Virol 2000;74:11347–58.
83. Zhang J, Yamada O, Yoshida H, Iwai T, Araki H. Autogenous translational inhibition of core protein: implication for switch from translation to RNA replication in hepatitis C virus. Virology 2002;293:141–50.
84. Li D, Takyar ST, Lott WB, Gowans EJ. Amino acids 1–20 of the hepatitis C virus (HCV) core protein specifically inhibit HCV IRES-dependent translation in HepG2 cells, and inhibit both HCV IRES- and cap-dependent translation in HuH7 and CV-1 cells. J Gen Virol 2003;84:815–25.
85. Friebe P, Lohmann V, Krieger N, Bartenschlager R. Sequences in the 5′ nontranslated region of hepatitis C virus required for RNA replication. J Virol 2001;75:12047–57.
86. Hüssy P, Langen H, Mous J, Jacobsen H. Hepatitis C virus core protein: carboxy-terminal boundaries of two processed species suggest cleavage by a signal peptide peptidase. Virology 1996;224: 93–104.
87. McLauchlan J, Lemberg MK, Hope G, Martoglio B. Intramembrane proteolysis promotes trafficking of hepatitis C virus core protein to lipid droplets. EMBO J 2002;21:3980–8.
88. Lemberg MK, Martoglio B. Requirements for signal peptide peptidase-catalyzed intramembrane proteolysis. Mol Cell 2002; 10:735–44.
89. Okamoto K, Moriishi K, Miyamura T, Matsuura Y. Intramembrane proteolysis and endoplasmic reticulum retention of hepatitis C virus core protein. J Virol 2004;78:6370–80.
90. Weihofen A, Binns K, Lemberg MK, Ashman K, Martoglio B. Identification of signal peptide peptidase, a presenilin-type aspartic protease. Science 2002;296:2215–8.
91. Pallaoro M, Lahm A, Biasiol G, Brunetti M, Nardella C, Orsatti L, et al. Characterization of the hepatitis C virus NS2/3 processing reaction by using a purified precursor protein. J Virol 2001;75: 9939–46.
92. Thibeault D, Maurice R, Pilote L, Lamarre D, Pause A. In vitro characterization of a purified NS2/3 protease variant of hepatitis C virus. J Biol Chem 2001;276:46678–84.
93. Bartenschlager R, Ahlborn-Laake L, Mous J, Jacobsen H. Kinetic and structural analyses of hepatitis C virus polyprotein processing. J Virol 1994;68:5045–55.
94. Failla C, Tomei L, De Francesco R. An amino-terminal domain of the hepatitis C virus NS3 protease is essential for interaction with NS4A. J Virol 1995;69:1769–77.
95. Lin C, Pragai BM, Grakoui A, Xu J, Rice CM. Hepatitis C virus NS3 serine proteinase: *trans*-cleavage requirements and processing kinetics. J Virol 1994;68:8147–57.
96. Tanji Y, Hijikata M, Hirowatari Y, Shimotohno K. Hepatitis C virus polyprotein processing: kinetics and mutagenic analysis of serine proteinase-dependent cleavage. J Virol 1994;68:8418–22.
97. Jin L, Peterson DL. Expression, isolation, and characterization of the hepatitis C virus ATPase/RNA helicase. Arch Biochem Biophys 1995;323:47–53.
98. Kim DW, Gwack Y, Han JH, Choe J. C-terminal domain of the hepatitis C virus NS3 protein contains an RNA helicase activity. Biochem Biophys Res Commun 1995;215:160–6.
99. Suzich JA, Tamura JK, Palmer-Hill F, Warrener P, Grakoui A, Rice CM, et al. Hepatitis C virus NS3 protein polynucleotide-stimulated nucleoside triphosphatase and comparison with the related pestivirus and flavivirus enzymes. J Virol 1993;67: 6152–8.

100. Tai CL, Chi WK, Chen DS, Hwang LH. The helicase activity associated with hepatitis C virus nonstructural protein 3 (NS3). J Virol 1996;70:8477–84.
101. Tai CL, Pan WC, Liaw SH, Yang UC, Hwang LH, Chen DS. Structure-based mutational analysis of the hepatitis C virus NS3 helicase. J Virol 2001;75:8289–97.
102. Wolk B, Sansonno D, Krausslich HG, Dammacco F, Rice CM, Blum HE, et al. Subcellular localization, stability, and trans-cleavage competence of the hepatitis C virus NS3–NS4A complex expressed in tetracycline-regulated cell lines. J Virol 2000;74:2293–304.
103. Barbato G, Cicero DO, Nardi MC, Steinkuhler C, Cortese R, De Francesco R, et al. The solution structure of the N-terminal proteinase domain of the hepatitis C virus (HCV) NS3 protein provides new insights into its activation and catalytic mechanism. J Mol Biol 1999;289:371–84.
104. Tanji Y, Hijikata M, Satoh S, Kaneko T, Shimotohno K. Hepatitis C virus-encoded nonstructural protein NS4A has versatile functions in viral protein processing. J Virol 1995;69:1575–81.
105. Restrepo-Hartwig MA, Ahlquist P. Brome mosaic virus helicase- and polymerase-like proteins colocalize on the endoplasmic reticulum at sites of viral RNA synthesis. J Virol 1996;70: 8908–16.
106. Schaad MC, Jensen PE, Carrington JC. Formation of plant RNA virus replication complexes on membranes: role of an endoplasmic reticulum-targeted viral protein. EMBO J 1997;16:4049–59.
107. van der Meer Y, van Tol H, Locker JK, Snijder EJ. ORF1a-encoded replicase subunits are involved in the membrane association of the arterivirus replication complex. J Virol 1998;72: 6689–98.
108. Shi ST, Schiller JJ, Kanjanahaluethai A, Baker SC, Oh JW, Lai MM. Colocalization and membrane association of murine hepatitis virus gene 1 products and de novo-synthesized viral RNA in infected cells. J Virol 1999;73:5957–69.
109. Froshauer S, Kartenbeck J, Helenius A. Alphavirus RNA replicase is located on the cytoplasmic surface of endosomes and lysosomes. J Cell Biol 1988;107:2075–86.
110. Egger D, Wolk B, Gosert R, Bianchi L, Blum HE, Moradpour D, et al. Expression of hepatitis C virus proteins induces distinct membrane alterations including a candidate viral replication complex. J Virol 2002;76:5974–84.
111. Gosert R, Egger D, Lohmann V, Bartenschlager R, Blum HE, Bienz K, et al. Identification of the hepatitis C virus RNA replication complex in Huh-7 cells harboring subgenomic replicons. J Virol 2003;77:5487–92.
112. Shi ST, Lee KJ, Aizaki H, Hwang SB, Lai MM. Hepatitis C virus RNA replication occurs on a detergent-resistant membrane that cofractionates with caveolin-2. J Virol 2003;77:4160–8.
113. Piccininni S, Varaklioti A, Nardelli M, Dave B, Raney KD, McCarthy JE. Modulation of the hepatitis C virus RNA-dependent RNA polymerase activity by the non-structural (NS) 3 helicase and the NS4B membrane protein. J Biol Chem 2002;277: 45670–9.
114. Gao L, Aizaki H, He JW, Lai MM. Interactions between viral nonstructural proteins and host protein hVAP-33 mediate the formation of hepatitis C virus RNA replication complex on lipid raft. J Virol 2004;78:3480–8.
115. Brass V, Bieck E, Montserret R, Wolk B, Hellings JA, Blum HE, et al. An amino-terminal amphipathic alpha-helix mediates membrane association of the hepatitis C virus nonstructural protein 5A. J Biol Chem 2002;277:8130–9.
116. Shimakami T, Hijikata M, Luo H, Ma YY, Kaneko S, Shimotohno K, et al. Effect of interaction between hepatitis C virus NS5A and NS5B on hepatitis C virus RNA replication with the hepatitis C virus replicon. J Virol 2004;78:2738–48.
117. Hamamoto I, Nishimura Y, Okamoto T, Aizaki H, Liu M, Mori Y, et al. Human VAP-B is involved in hepatitis C virus replication through interaction with NS5A and NS5B. J Virol 2005;79: 13473–82.
118. Ito T, Lai MM. An internal polypyrimidine-tract-binding protein-binding site in the hepatitis C virus RNA attenuates translation, which is relieved by the 3′-untranslated sequence. Virology 1999;254:288–96.
119. Kolykhalov AA, Agapov EV, Blight KJ, Mihalik K, Feinstone SM, Rice CM. Transmission of hepatitis C by intrahepatic inoculation with transcribed RNA. Science 1997;277:570–4.
120. Tanaka T, Kato N, Cho M-J, Shimotohno K. A novel sequence found at the 3′ terminus of hepatitis C virus genome. Biochem Biophys Res Commun 1995;215:744–9.
121. Yi M, Lemon SM. 3′ nontranslated RNA signals required for replication of hepatitis C virus RNA. J Virol 2003;77:3557–68.
122. Friebe P, Bartenschlager R. Genetic analysis of sequences in the 3′ nontranslated region of hepatitis C virus that are important for RNA replication. J Virol 2002;76:5326–38.
123. Aizaki H, Lee KJ, Sung VM, Ishiko H, Lai MM. Characterization of the hepatitis C virus RNA replication complex associated with lipid rafts. Virology 2004;324:450–61.
124. Ali N, Tardif KD, Siddiqui A. Cell-free replication of the hepatitis C virus subgenomic replicon. J Virol 2002;76:12001–7.
125. Lai VC, Dempsey S, Lau JY, Hong Z, Zhong W. In vitro RNA replication directed by replicase complexes isolated from the subgenomic replicon cells of hepatitis C virus. J Virol 2003;77: 2295–300.
126. Miyanari Y, Hijikata M, Yamaji M, Hosaka M, Takahashi H, Shimotohno K. Hepatitis C virus non-structural proteins in the probable membranous compartment function in viral genome replication. J Biol Chem 2003;278:50301–8.
127. Hardy RW, Marcotrigiano J, Blight KJ, Majors JE, Rice CM. Hepatitis C virus RNA synthesis in a cell-free system isolated from replicon-containing hepatoma cells. J Virol 2003;77: 2029–37.
128. Waris G, Sarker S, Siddiqui A. Two-step affinity purification of the hepatitis C virus ribonucleoprotein complex. RNA 2004;10: 321–9.
129. Simons K, Ikonen E. Functional rafts in cell membranes. Nature 1997;387:569–72.
130. Simons K, Ikonen E. How cells handle cholesterol. Science 2000;290:1721–6.
131. Simons K, Toomre D. Lipid rafts and signal transduction. Nat Rev Mol Cell Biol 2000;1:31–9.
132. Barman S, Ali A, Hui EK, Adhikary L, Nayak DP. Transport of viral proteins to the apical membranes and interaction of matrix protein with glycoproteins in the assembly of influenza viruses. Virus Res 2001;77:61–9.
133. Scheiffele P, Rietveld A, Wilk T, Simons K. Influenza viruses select ordered lipid domains during budding from the plasma membrane. J Biol Chem 1999;274:2038–44.
134. Zhang J, Pekosz A, Lamb RA. Influenza virus assembly and lipid raft microdomains: a role for the cytoplasmic tails of the spike glycoproteins. J Virol 2000;74:4634–44.
135. Ding L, Derdowski A, Wang JJ, Spearman P. Independent segregation of human immunodeficiency virus type 1 Gag protein complexes and lipid rafts. J Virol 2003;77:1916–26.
136. Ono A, Freed EO. Plasma membrane rafts play a critical role in HIV-1 assembly and release. Proc Natl Acad Sci USA 2001;98: 13925–30.
137. Bavari S, Bosio CM, Wiegand E, Ruthel G, Will AB, Geisbert TW, et al. Lipid raft microdomains: a gateway for compartmentalized trafficking of Ebola and Marburg viruses. J Exp Med 2002;195:593–602.
138. Stuart AD, Eustace HE, McKee TA, Brown TD. A novel cell entry pathway for a DAF-using human enterovirus is dependent on lipid rafts. J Virol 2002;76:9307–22.
139. Narayan S, Barnard RJ, Young JA. Two retroviral entry pathways distinguished by lipid raft association of the viral receptor and differences in viral infectivity. J Virol 2003;77: 1977–83.

140. Ashbourne Excoffon KJ, Moninger T, Zabner J. The Coxsackie B virus and adenovirus receptor resides in a distinct membrane microdomain. J Virol 2003;77:2559–67.
141. Brown DA, Rose JK. Sorting of GPI-anchored proteins to glycolipid-enriched membrane subdomains during transport to the apical cell surface. Cell 1992;68:533–44.
142. Hijikata M, Mizushima H, Tanji Y, Komoda Y, Hirowatari Y, Akagi T, et al. Proteolytic processing and membrane association of putative nonstructural proteins of hepatitis C virus. Proc Natl Acad Sci USA 1993;90:10773–7.
143. Mottola G, Cardinali G, Ceccacci A, Trozzi C, Bartholomew L, Torrisi MR, et al. Hepatitis C virus nonstructural proteins are localized in a modified endoplasmic reticulum of cells expressing viral subgenomic replicons. Virology 2002;293:31–43.
144. Tu H, Gao L, Shi ST, Taylor DR, Yang T, Mircheff AK, et al. Hepatitis C virus RNA polymerase and NS5A complex with a SNARE-like protein. Virology 1999;263:30–41.
145. Pietschmann T, Lohmann V, Rutter G, Kurpanek K, Bartenschlager R. Characterization of cell lines carrying self-replicating hepatitis C virus RNAs. J Virol 2001;75:1252–64.
146. Choi J, Lee KJ, Zheng Y, Yamaga AK, Lai MM, Ou JH. Reactive oxygen species suppress hepatitis C virus RNA replication in human hepatoma cells. Hepatology 2004;39:81–9.
147. Kaito M, Watanabe S, Tsukiyama-Kohara K, Yamaguchi K, Kobayashi Y, Konishi M, et al. Hepatitis C virus particle detected by immunoelectron microscopic study. J Gen Virol 1994; 75:1755–60.
148. Shimizu YK, Feinstone SM, Kohara M, Purcell RH, Yoshikura H. Hepatitis C virus: detection of intracellular virus particles by electron microscopy. Hepatology 1996;23:205–9.
149. Maillard P, Krawczynski K, Nitkiewicz J, Bronnert C, Sidorkiewicz M, Gounon P, et al. Nonenveloped nucleocapsids of hepatitis C virus in the serum of infected patients. J Virol 2001;75: 8240–50.
150. Andre P, Komurian-Pradel F, Deforges S, Perret M, Berland JL, Sodoyer M, et al. Characterization of low- and very-low-density hepatitis C virus RNA-containing particles. J Virol 2002;76: 6919–28.
151. Moradpour D, Wakita T, Tokushige K, Carlson RI, Krawczynski K, Wands JR. Characterization of three novel monoclonal antibodies against hepatitis C virus core protein. J Med Virol 1996;48: 234–41.
152. Barba G, Harper F, Harada T, Kohara M, Goulinet S, Matsuura Y, et al. Hepatitis C virus core protein shows a cytoplasmic localization and associates to cellular lipid storage droplets. Proc Natl Acad Sci USA 1997;94:1200–5.
153. Moriya K, Fujie H, Shintani Y, Yotsuyanagi H, Tsutsumi T, Ishibashi K, et al. The core protein of hepatitis C virus induces hepatocellular carcinoma in transgenic mice. Nat Med 1998;4: 1065–7.
154. Hope RG, Murphy DJ, McLauchlan J. The domains required to direct core proteins of hepatitis C virus and GB virus-B to lipid droplets share common features with plant oleosin proteins. J Biol Chem 2002;277:4261–70.
155. Suzuki R, Sakamoto S, Tsutsumi T, Rikimaru A, Tanaka K, Shimoike T, et al. Molecular determinants for subcellular localization of hepatitis C virus core protein. J Virol 2005;79: 1271–81.
156. Suzuki T, Suzuki R. Maturation and assembly of hepatitis C virus core protein. In: Kalitzky M, Borowski P, editors. Molecular biology of the Flavivirus. Norfolk, UK: Horizon Bioscience; 2006. p. 295–311.
157. Shintani Y, Fujie H, Miyoshi H, Tsutsumi T, Tsukamoto K, Kimura S, et al. Hepatitis C virus infection and diabetes: direct involvement of the virus in the development of insulin resistance. Gastroenterology 2004;126:840–8.
158. Moriishi K, Mochizuki R, Moriya K, Miyamoto H, Mori Y, Abe T, et al. Critical role of PA28γ in hepatitis C virus-associated steatogenesis and hepatocarcinogenesis. Proc Natl Acad Sci U S A 2007;104:1661–6.
159. Miyamoto H, Moriishi K, Moriya K, Murata S, Tanaka K, Suzuki T, et al. Involvement of the PA28γ-dependent pathway in insulin resistance induced by hepatitis C virus core protein. J Virol 2007;81:1727–35.
160. Nakai K, Okamoto T, Kimura-Someya T, Ishii K, Lim CK, Tani H, et al. Oligomerization of hepatitis C virus core protein is crucial for interaction with the cytoplasmic domain of E1 envelope protein. J Virol 2006;80:11265–73.
161. Baumert TF, Ito S, Wong DT, Liang TJ. Hepatitis C virus structural proteins assemble into viruslike particles in insect cells. J Virol 1998;72:3827–36.
162. Falcon V, Garcia C, de la Rosa MC, Menendez I, Seoane J, Grillo JM. Ultrastructural and immunocytochemical evidences of core-particle formation in the methylotrophic *Pichia pastoris* yeast when expressing HCV structural proteins (core-E1). Tissue Cell 1999;31:117–25.
163. Kunkel M, Lorinczi M, Rijnbrand R, Lemon SM, Watowich SJ. Self-assembly of nucleocapsid-like particles from recombinant hepatitis C virus core protein. J Virol 2001;75:2119–29.
164. Lorenzo LJ, Duenas-Carrera S, Falcon V, Acosta-Rivero N, Gonzalez E, de la Rosa MC, et al. Assembly of truncated HCV core antigen into virus-like particles in *Escherichia coli*. Biochem Biophys Res Commun 2001;281:962–5.
165. Acosta-Rivero N, Aguilar JC, Musacchio A, Falcon V, Vina A, de la Rosa MC, et al. Characterization of the HCV core virus-like particles produced in the methylotrophic yeast *Pichia pastoris*. Biochem Biophys Res Commun 2001;287:122–5.
166. Kunkel M, Watowich SJ. Conformational changes accompanying self-assembly of the hepatitis C virus core protein. Virology 2002;294:239–45.
167. Acosta-Rivero N, Falcon V, Alvarez C, Musacchio A, Chinea G, Cristina de la Rosa M, et al. Structured HCV nucleocapsids composed of P21 core protein assemble primary in the nucleus of *Pichia pastoris* yeast. Biochem Biophys Res Commun 2003; 310:48–53.
168. Blanchard E, Hourioux C, Brand D, Ait-Goughoulte M, Moreau A, Trassard S, et al. Hepatitis C virus-like particle budding: role of the core protein and importance of its Asp111. J Virol 2003; 77:10131–8.
169. Majeau N, Gagne V, Boivin A, Bolduc M, Majeau JA, Ouellet D, et al. The N-terminal half of the core protein of hepatitis C virus is sufficient for nucleocapsid formation. J Gen Virol 2004; 85:971–81.
170. Klein KC, Polyak SJ, Lingappa JR. Unique features of hepatitis C virus capsid formation revealed by de novo cell-free assembly. J Virol 2004;78:9257–69.
171. Kunkel M, Watowich SJ. Biophysical characterization of hepatitis C virus core protein: implications for interactions within the virus and host. FEBS Lett 2004;557:174–80.
172. Matsumoto M, Hwang SB, Jeng KS, Zhu N, Lai MM. Homotypic interaction and multimerization of hepatitis C virus core protein. Virology 1996;218:43–51.
173. Nolandt O, Kern V, Muller H, Pfaff E, Theilmann L, Welker R, et al. Analysis of hepatitis C virus core protein interaction domains. J Gen Virol 1997;78(Pt 6):1331–40.
174. Yan BS, Tam MH, Syu WJ. Self-association of the C-terminal domain of the hepatitis-C virus core protein. Eur J Biochem 1998;258:100–6.
175. Ezelle HJ, Markovic D, Barber GN. Generation of hepatitis C virus-like particles by use of a recombinant vesicular stomatitis virus vector. J Virol 2002;76:12325–34.
176. Clayton RF, Owsianka A, Aitken J, Graham S, Bhella D, Patel AH. Analysis of antigenicity and topology of E2 glycoprotein present on recombinant hepatitis C virus-like particles. J Virol 2002;76:7672–82.
177. Lo S-Y, Selby MJ, Ou J-H. Interaction between hepatitis C virus core protein and E1 envelope protein. J Virol 1996;70:5177–82.

178. Ma HC, Ke CH, Hsieh TY, Lo SY. The first hydrophobic domain of the hepatitis C virus E1 protein is important for interaction with the capsid protein. J Gen Virol 2002;83:3085–92.
179. Hershko A, Ciechanover A. The ubiquitin system. Annu Rev Biochem 1998;67:425–79.
180. Finley D, Ciechanover A, Varshavsky A. Ubiquitin as a central cellular regulator. Cell 2004;116:S29–32, 2 p following S.
181. Suzuki R, Tamura K, Li J, Ishii K, Matsuura Y, Miyamura T, et al. Ubiquitin-mediated degradation of hepatitis C virus core protein is regulated by processing at its carboxyl terminus. Virology 2001;280:301–9.
182. Moriishi K, Okabayashi T, Nakai K, Moriya K, Koike K, Murata S, et al. Proteasome activator PA28γ-dependent nuclear retention and degradation of hepatitis C virus core protein. J Virol 2003;77:10237–49.
183. Shirakura M, Murakami K, Ichimura T, Suzuki R, Shimoji T, Fukuda K, et al. E6AP ubiquitin ligase mediates ubiquitylation and degradation of hepatitis C virus core protein. J Virol 2007; 81:1174–85.
184. Huibregtse JM, Scheffner M, Beaudenon S, Howley PM. A family of proteins structurally and functionally related to the E6-AP ubiquitin–protein ligase. Proc Natl Acad Sci USA 1995;92: 2563–7.
185. Huibregtse JM, Scheffner M, Howley PM. Cloning and expression of the cDNA for E6-AP, a protein that mediates the interaction of the human papillomavirus E6 oncoprotein with p53. Mol Cell Biol 1993;13:775–84.
186. Scheffner M, Huibregtse JM, Vierstra RD, Howley PM. The HPV-16 E6 and E6-AP complex functions as a ubiquitin-protein ligase in the ubiquitination of p53. Cell 1993;75:495–505.
187. Tanahashi N, Yokota K, Ahn JY, Chung CH, Fujiwara T, Takahashi E, et al. Molecular properties of the proteasome activator PA28 family proteins and gamma-interferon regulation. Genes Cells 1997;2:195–211.
188. Realini C, Jensen CC, Zhang Z, Johnston SC, Knowlton JR, Hill CP, et al. Characterization of recombinant REGalpha, REGbeta, and REGgamma proteasome activators. J Biol Chem 1997;272:25483–92.
189. Polyak SJ, Klein KC, Shoji I, Miyamura T, Lingappa JR. Assemble and interact pleiotropic functions of the HCV core protein. In: Tan S-L, editor. Hepatitis C viruses: genomes and molecular biology. Norwich, UK: Horizon Bioscience; 2006. p. 89–119.

Available online at www.sciencedirect.com
ScienceDirect
Journal of Virological Methods 148 (2008) 174–181
Journal of Virological Methods
www.elsevier.com/locate/jviromet

Dynamic behavior of hepatitis C virus quasispecies in a long-term culture of the three-dimensional radial-flow bioreactor system

Kyoko Murakami [a], Yasushi Inoue [a,b], Su-Su Hmwe [a,c], Kazuhiko Omata [a,d], Tomokatsu Hongo [e], Koji Ishii [a], Sayaka Yoshizaki [a], Hideki Aizaki [a], Tomokazu Matsuura [f], Ikuo Shoji [a], Tatsuo Miyamura [a], Tetsuro Suzuki [a,*]

[a] *Department of Virology II, National Institute of Infectious Diseases, 1-23-1 Toyama, Shinjuku-ku, Tokyo 162-8640, Japan*
[b] *Pulmonary and Critical Care Unit, Mita Hospital, International University of Health and Welfare, Japan*
[c] *Department of Infectious Diseases, Internal Medicine, Graduate School of Medicine, University of Tokyo, Tokyo, Japan*
[d] *Department of Oral and Maxillofacial Surgery, The Nippon Dental University School of Dentistry at Tokyo, Tokyo, Japan*
[e] *ABLE Corporation, Shizuoka, Japan*
[f] *Department of Laboratory medicine, The Jikei University School of Medicine, Tokyo, Japan*

Received 25 July 2007; received in revised form 9 November 2007; accepted 21 November 2007

Abstract

Hepatitis C virus (HCV) exists in infected individuals as quasispecies, usually consisting of a dominant viral isolate and a variable mixture of related, yet genetically distinct, variants. A prior HCV infection system was developed using human hepatocellular carcinoma cells cultured in the three-dimensional radial-flow bioreactor (RFB), in which the cells retain morphological appearance and their differentiated hepatocyte functions for an extended period of time. This report studies the selection and alteration of the viral quasispecies in the RFB system inoculated with pooled serum derived from HCV carriers. Monitoring the viral RNA and core protein in the culture supernatants, together with nucleotide sequencing of hypervariable region 1 of the HCV genome, demonstrated that (1) the virus production intermittently fluctuated in the cultures, (2) the viral genetic diversity was markedly reduced 3 days post-infection (p.i.), and (3) dominant species changed on days 19–33 p.i., suggesting that the virus populations can be selected according to susceptibility to the viral infection and replication. A therapeutic effect of interferon-α also demonstrated the inhibition of HCV expression. Thus, this HCV infection model in the RFB system should be useful for investigating the dynamic behavior of HCV quasispecies in cultured cells and evaluating anti-HCV compounds.

Keywords: Hepatitis C virus; Three-dimensional culture; Radial-flow bioreactor; Dynamics; Quasispecies

1. Introduction

Hepatitis C virus (HCV) is a major cause of chronic liver diseases (Choo et al., 1989; Kuo et al., 1989; Saito et al., 1990) and has been estimated to infect more than 170 million people throughout the world (Poynard et al., 2003). Symptoms of persistent HCV infection extend from chronic hepatitis to cirrhosis and ultimately hepatocellular carcinoma (Choo et al., 1989; Kuo et al., 1989; Saito et al., 1990). HCV belongs to the genus *Hepacivirus*, included in the family of Flaviviridae, and possesses a viral genome of a single, positive-stranded RNA with a nucleotide (nt) length of approximately 9.6 kb (Choo et al., 1991; Grakoui et al., 1993; Hijikata et al., 1991). It has been shown that HCV, like many other RNA viruses, circulates within infected individuals as a diverse population and closely related variants are referred to as quasispecies (Martell et al., 1992). This quasispecies model of mixed virus populations may imply a significant survival advantage because the simultaneous presence of multiple variant genomes and/or high rate of generation of new variants allow rapid selection of the mutants are better suited to new environmental conditions (Pawlotsky, 2006).

Studies on HCV replication and development of selective antiviral drugs have been hampered primarily by the lack of efficient cell culture systems. Establishment of selectable dicistronic HCV RNAs that are capable of autonomous replication to high levels in human hepatoma Huh-7 cells was a

* Corresponding author. Tel.: +81 3 5285 1111; fax: +81 3 5285 1161.
E-mail address: tesuzuki@nih.go.jp (T. Suzuki).

0166-0934/$ – see front matter © 2007 Elsevier B.V. All rights reserved.
doi:10.1016/j.jviromet.2007.11.001

significant breakthrough in HCV research; however, virus production has not been observed in the conventional monolayer cultures (Blight et al., 2000; Lohmann et al., 1999). Recently, it has been described that infectious HCV particles are efficiently produced from a genotype 2a isolate JFH-1 in Huh-7 cells (Blight et al., 2000; Wakita et al., 2005; Zhong et al., 2005). This JFH-1 based HCV culture system is an invaluable achievement permitting a variety of studies on the complete HCV life cycle. However, HCV infection systems with human sera or plasmas containing intact virions are still limited because of low levels of propagation in the cultures. Reverse transcription (RT)-PCR was typically used to detect the viral RNA in cell extracts; however, synthesized viral proteins were not observed in these systems (Ikeda et al., 1998; Tagawa et al., 1995).

There are reports of differentiated human hepatoma FLC4 (functional liver cell 4) cells grown in a three-dimensional (3D) radial-flow bioreactor (RFB) that can be infected by HCV-positive serum and support viral replication (Aizaki et al., 2003). Furthermore, production and release of infectious HCV has been observed in the RFB system following transfection of FLC4 cells with *in vitro* transcribed HCV genomic RNA, as well as in a 3D system using Huh-7 cells harboring genome-length dicistronic RNAs (Murakami et al., 2006). The RFB system, in which the bioreactor column consists of a cylindrical matrix with porous bead microcarriers extended vertically, was aimed initially at developing artificial liver tissues and allows liver-derived cells to maintain morphological appearance as well as their physiological functions, such as the ability to synthesize albumin and drug-metabolizing activity mediated by cytochrome P450 (Iwahori et al., 2003). The radial-flow configuration permits full contact between culture medium and cells at a physiologic perfusion flow rate, and prevents excessive shear stresses and buildup of waste products, thus ensuring the long-term viability of 3D cell culture.

The aim of the present study was to characterize HCV dynamics in the RFB system during long-term cultures inoculated with pooled serum obtained from HCV carriers, and to examine the therapeutic effects of interferon-alpha (IFN-α) in this HCV infection model.

2. Materials and methods

2.1. Cell cultures

FLC4 cells (Aoki et al., 1998), which were derived from human hepatocellular carcinoma cells and negative for HCV RNA and HBV DNA, were maintained in serum-free ASF104 medium (Ajinomoto, Japan) supplemented with 4 g/L D-glucose on the collagen-coated dishes before inoculating into the RFB column. The RFB system (ABLE, Japan) was manipulated as described previously (Aizaki et al., 2003) with minor modifications. Briefly, RFB columns, which have bed volumes of 30 or 4 mL and are filled with porous glass microcarriers (diameter 0.6 mm, vacant capacity 50%, pore size <120 μm) (Hongo et al., 2005), were seeded with FLC4 cells, which subsequently attached to the surface and inside of porous glass beads. ASF104 medium containing 2% fetal calf serum was added at a flow rate of 50 mL/day, and the culture condition was automatically controlled by monitoring temperature, pH value and oxygen levels in the vessel throughout the duration of the study.

2.2. Infection of HCV-positive sera

HCV antibody-positive sera used in this study were blood donor samples supplied by The Japanese Red Cross Center, Tokyo, Japan. HCV RNA loads in the sera were as follows: serum A, 2.4×10^6 copies/mL; serum B, 8.6×10^6 copies/mL; serum C, 5.9×10^6 copies/mL; serum D, 2.5×10^6 copies/mL; serum E, 1.0×10^7 copies/mL; serum F, 1.4×10^7 copies/mL (Table 1). In the first experiment (Fig. 3), aliquots of each serum containing 2×10^6 copies of HCV RNA were mixed and pooled serum sample with 1.2×10^7 copies was prepared as an inoculum. The pooled serum (2.5 mL) was added to the 3D cultured-FLC4 cells in the 30-mL RFB column, and the culture medium was changed after 12 h of incubation. At various times during the culture period, culture medium (50 mL) was collected to determine HCV RNA and the core protein. Collected culture media were passed through a 0.20-μm filter to remove the debris, and stored at −80 °C. In the second experiment to evaluate a therapeutic effect of anti-HCV drug (Fig. 4), 4-mL RFB columns were used. IFN-α (Sumiferon 300; Sumitomo Pharmaceuticals, Japan) was added to one of two columns at a final concentration of 100 IU/mL after the infection. Culture medium was periodically collected for determination of HCV RNA, the core protein and transaminases, and was replaced with the same volume of fresh medium with or without IFN-α.

2.3. Quantitation of HCV RNA and core protein

HCV RNA was extracted from 140 μL of each serum or culture medium using QIAamp Viral RNA Mini spin column (QIAGEN); RNA was eluted in 60 μL of water and stored at −80 °C. Real-time RT-PCR was performed using TaqMan EZ RT-PCR Core Reagents (PE Applied Biosystems), as described previously (Aizaki et al., 2003; Suzuki et al., 2005). The viral core antigen in the culture medium was quantified by immunoassay (Ortho HCV-Core ELISA Kit; Ortho-Clinical Diagnotics), according to the manufacturer's instruction (Murakami et al., 2006).

2.4. PCR amplification and nucleotide sequencing of HVR1 domain and its flanking region

Five microliters of RNA samples prepared as above were reverse transcribed using SuperScript II (Invitrogen) and a specific primer 5′-CATCCATGTGCAGCCGAACC-3′ (corresponding to nucleotides [nt] 2006–1987 of HCV NIHJ1) (Aizaki et al., 1998). For the nested PCR, a genotype-independent set of primers specific for hypervariable region 1 (HVR1). The first round of PCR was performed with the outer sense primer 5′-GCATGGCTTGGGATATGATG-3′ (nt 1291–1310) and with the reverse transcription primer described above as the outer antisense primer. After the initial 3.5-min denaturation step at 94 °C, 35 PCR cycles, with each cycle

Table 1
HCV-positive sera used in this study

Serum	Clone	HCV HVR1 sequence	% in the serum	genotype
A	A1	KVLIVMLSFAGVDGSTRTIGGRTAHTTQGSASLFSSGPAQKIQLINTNGS	75	1
	A2	-------L------N-H-V--AV-SS---FT---KL----------S---	12.5	
	A3	-------L------N-YAS---AGLL-R-V--I-TA----------S---	12.5	
B	B1	KVVVILLLAAGVDAGTNTIGGSAAQTTSGFTGLFRSGARQNIQLINTNGS	50	2
	B2	----------R	12.5	
	B3	----------S---------	12.5	
	B4	--L-V---F-----E-HVT--N-GR--A-LV--LTP--K----------	12.5	
	B5	--I----------	12.5	
C	C1	KVLIVMLLFAGVDGDTHVSGGTQGRAAYGLASLFALGPTQKIQLVNTNGS	83.3	1
	C2	----------A----------	16.7	
D	D1	KVLIVMLLFAGVDGVTHTSGAAAGHNARSLSGLFSLGSAQKLQLINTNGS	40	1
	D2	----------A-Y---GT--Y-TKTFT-F--R-PS--I--------	20	
	D3	----------T--Y---T-T----P--------V-----	10	
	D4	----------V---T----P--------V-----	10	
	D5	----------V-----	10	
	D6	----------Y-T--FT----S-----I--V-----	10	
E	E1	KVLIVMLLFAGVDGSTRVSGGQAGRVTKSLASFFSPGPQQKIQLVNSNGS	40	1
	E2	----------HGFT-L--A-S----------	30	
	E3	----------QGFT-L--A-S----------	10	
	E4	----------S-FT-L-TV----------	10	
	E5	----------N-Y---------AH--T-L--A-S----------	10	
F	F1	KVLIVMLLFAGVDGETNVMGGRAGHTTNTFTSLFSVGPAQKIQLVNSNGS	37	1
	F2	----------D-K----------S-L----N---S----------	27	
	F3	----------K----Q-----S-L----N---S----------	18	
	F4	----------A-------A--TK---------D----	9	
	F5	----------G--------A--A--L----TR--S----------	9	

consisting of 1 min at 94 °C, 2 min at 45 °C, and 3 min at 72 °C, were carried out, followed by a 10-min extension step at 72 °C. The second round was performed with the inner sense primer 5′-GGTAAGCTTTCCATGGTGGGGAACTGGGC-3′ (nt 1419–1447) and the inner antisense primer 5′-CTGGAATTCGCAGTCCTGTTGATGTGCCA-3′ (nt 1627–1599). The amplified products were cloned into the pGEM-T vector (Promega), and at least 8 independent clones were sequenced with an automatic DNA sequencer (ABI PRISM 310, PE Applied Biosystems).

3. Results

3.1. The outline of the RFB system

The RFB system was initially aimed at developing artificial liver tissues and allows liver-derived cells to maintain morphological appearance as well as their physiological functions, such as the ability to synthesize albumin and drug-metabolizing activity mediated by cytochrome P450 (Iwahori et al., 2003). Fig. 1 shows the outline of the RFB system. The bioreactor column consists of a vertically extended cylindrical matrix with porous glass microcarriers, which were most suitable for FLC4 culture as described in Section 2. The conditioning vessel is connected to a circulation system including tanks either for supplying fresh medium or for recovering sample aliquots. Oxygen consumption, temperature and pH of the culture medium are monitored continuously and conditioned in the vessel by computer and mass flow controller throughout the culture. Thus, the radial-flow configuration permits full contact between culture medium and cells at a physiologic perfusion flow rate, and prevents excessive shear stresses and a buildup of waste products, thus ensuring the long-term viability of 3D culture. For the long-term culture up to 110 days, temperature in the vessel gradually decreased from 37 to 30 °C as shown in Fig. 2A. The oxygen consumption, which indicates the cell growth condition, increased slowly from days 0 to 80 post-inoculation of the cells, and maintained a constant level afterwards. Under this condition, the production rate of albumin was found to be stable from days 15 to 105. The following experiments of HCV infection were done in such a stable phase of the cell condition after 3 weeks of pre-culture. Cell grown in the RFB column reached confluence at the end of culture (day 110) since the cells were observed outside the matrix bed (Fig. 2B).

3.2. Infection of HCV-positive sera to RFB cultured FLC4 cells

Previously, HCV RNA could be detected in FLC4 cells grown in the RFB up to 4 weeks of culture following inoculation with an HCV carrier plasmid (Aizaki et al., 2003). Establishment of a long-term stable culture system of human liver-derived cells